ChemPubSoc Europe

DOI: 10.1002/cmdc.201402371

Identification of Structural Features of 2-Alkylidene-1,3-Dicarbonyl Derivatives that Induce Inhibition and/or Activation of Histone Acetyltransferases KAT3B/p300 and KAT2B/PCAF

Sabrina Castellano,[a] Ciro Milite,[a] Alessandra Feoli,[a] Monica Viviano,[a] Antonello Mai,[b] Ettore Novellino,[c] Alessandra Tosco,*[a] and Gianluca Sbardella*[a]

Dedicated to Prof. Marino Artico on the occasion of his 80th birthday.

Dysregulation of the activity of lysine acetyltransferases (KATs) is related to a variety of diseases and/or pathological cellular states; however, their role remains unclear. Therefore, the development of selective modulators of these enzymes is of paramount importance, because these molecules could be invaluable tools for assessing the importance of KATs in several pathologies. We recently found that diethyl pentadecylidenemalonate (SPV106) possesses a previously unobserved inhibitor/activator activity profile against protein acetyltransferases. Herein, we report that manipulation of the carbonyl functions of a series of analogues of SPV106 yielded different activity profiles against KAT2B and KAT3B (pure KAT2B activator, pan-inhibitor, or mixed KAT2B activator/KAT3B inhibitor). Among the novel compounds, a few derivatives may be useful chemical tools for studying the mechanism of lysine acetylation and its implications in physiological and/or pathological processes.

Introduction

Lysine acetylation was first identified nearly 50 years ago[1] and has gained interest over the past two decades. Through crosstalk with other prominent posttranslational modifications (e.g., iterative methylation),[2] lysine acetylation gives rise to a complex network, named the "histone code",[2b,3] that affects the structure of nucleosomes and is crucial for the modulation of chromatin-based transcriptional control and shaping inheritable epigenetic programs.[2a,4] In fact, gene regulation is correlated with the acetylation state of histones; transcriptionally repressed genes are associated with hypoacetylated histones, and transcriptionally active genes are associated with hyperacetylated histones. Similar crosstalk, named the "protein modification code,"[3a,5] between acetylation and other posttranslational modifications occurs in many non-histone proteins that have a diverse range of functions,[6] including transcription factors (i.e., p53),[7] other nuclear regulators (i.e., α-tubulin),[8] and cytoplasmic proteins.[5,9] As a result, lysine acetylation appears to have a crucial role not only in the nucleus but also in the regulation of different cytoplasmic processes, including cytoskeleton dynamics, energy metabolism, endocytosis, autophagy, and signaling from the plasma membrane.[10] Moreover, reversible lysine acetylation may alter enzymatic activity to allow cells to respond to environmental changes in metabolic demands, and it has been proposed to be an evolutionarily conserved mechanism for the regulation of cellular functions.[11]

The acetylation level of proteins is controlled by the action of lysine acetyltransferases (KATs)[12] and deacetylases (KDACs),[13] and its deregulation has been linked to several diseases and disorders, including cancer, inflammation and metabolic and neurodegenerative diseases.[14] A number of KDAC inhibitors are currently undergoing clinical evaluation for efficacy in the treatment of human tumors,[15] and two of these inhibitors, suberoylanilide hydroxamic acid (SAHA, vorinostat)[16] and FK228 (FR901228, romidepsin),[17] have been recently approved by the US Food and Drug Administration (FDA) for clinical use in refractory cutaneous T-cell lymphoma.

In contrast, KATs are less validated as chemotherapeutic targets. These enzymes can be organized into families (Figure 1) based on primary structure homology within the catalytic domain and the biochemical mechanism of acetyl transfer. Several KAT families have been identified, but only four have been extensively studied: the Gcn5-related N-acetyltransferase (GNAT) family (KAT2), the E1A-associated 300 kDa protein (p300)/CREB-binding protein (CBP) family (KAT3), the MYST

[a] Prof. Dr. S. Castellano, Dr. C. Milite, A. Feoli, Dr. M. Viviano, Prof. Dr. A. Tosco, Prof. Dr. G. Sbardella
Dipartimento di Farmacia, Università degli Studi di Salerno
Via Giovanni Paolo II 132, 84084 Fisciano (SA) (Italy)
E-mail: tosco@unisa.it
gsbardella@unisa.it

[b] Prof. Dr. A. Mai
Dipartimento di Chimica e Tecnologie del Farmaco
"Sapienza" Università di Roma, P.le A. Moro 5, 00185 Rome (Italy)

[c] Prof. E. Novellino
Dipartimento di Farmacia, Università di Napoli "Federico II"
Via D. Montesano 49, 80131 Naples (Italy)

Supporting information for this article is available on the WWW under http://dx.doi.org/10.1002/cmdc.201402371.

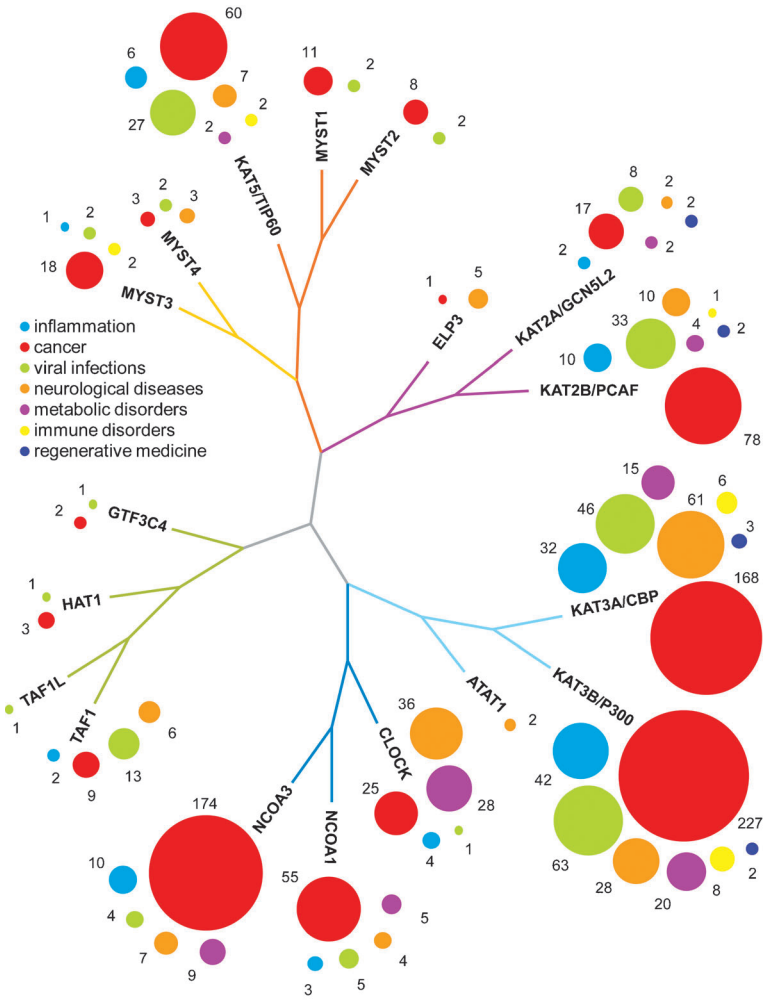

Figure 1. Phylogenetic tree of KAT enzymes and their relationships with diseases. The sizes of the colored circles represent the number of articles (according to NCBI PubMed at the date of manuscript submission) associated with a specific disease based on the presence of keywords in the abstract or MeSH terms of PubMed entries. This tree was obtained from the Structural Genomic Consortium ChromoHub[21] and modified with Adobe Illustrator CS5.

family (KAT6), and the regulation of Ty1 transposition gene product 109 (Rtt109) family (KAT11).[5, 12, 14c, 18]

Dysregulation of the activity of KAT enzymes has been related to a variety of diseases and/or pathological cellular states (infographic in Figure 1).[14] In particular, the GCN5/PCAF and CBP/p300 paralogue pairs have been pursued as potential therapeutic targets in cancer,[19] inflammation,[20] viral diseases,[18e, 20c] cardiomyopathies,[22] and disturbances in neuronal cell plasticity and differentiation.[23] However, at least in cancer, their role cannot be simply generalized, because they can function as either tumor suppressors or promoters depending on the tumor type and development stage.[11a, 14a] Therefore, cell-permeable, selective modulators of these enzymes may be important tools for reverse chemical genetics studies[24] and assessing the implication of KATs in several pathologies. Moreover, these modulators can represent starting points for the design of novel epigenetic drugs.

Different approaches have been used to identify KAT modulators,[14c] but only a limited number of small molecule inhibitors have been described (Figure 2), with various degrees of selectivity and cell permeability. Mechanism-based peptide–CoA conjugates (Lys–CoA and H3–CoA-20) have been reported as potent and selective bisubstrate inhibitors for KAT3B (p300) and KAT2B (PCAF). Unfortunately, these conjugates are not metabolically stable and have poor cell permeability.[23a, 25] Ethnomedicine has inspired the identification of a few natural products, including anacardic acid,[26] garcinol,[27] curcumin,[28] plumbagin,[29] and guttiferone A,[30] and some analogues[31] or semi-synthetic derivatives,[20c, 32] as inhibitors of different classes of KATs.

Isothiazolones[33] and pyridoisothiazolones[34] were reported to be cell-permeable, potent inhibitors of KAT2B, but their chemical reactivity (and limited solubility in the case of pyridoisothiazolones) limits their specificity. Recently, a virtual screening approach led to the identification of pyrazolone derivatives as selective KAT3B inhibitors.[24b, 35] Cell-permeable KAT2A (GCN5)-selective inhibitors, such as γ-butyrolactone MB-3[36] and a few quinoline derivatives,[37] have also been reported.

In addition to inhibitors, a few KAT enzyme activators have also been reported. For example, anacardic acid-inspired *N*-(4-chloro-3-trifluoromethyl-phenyl)-2-ethoxy-6-pentadecyl-benzamide (CTPB, Figure 3)[26] and garcinol-related nemorosone[30] were reported to selectively activate p300 HAT activity. Interestingly, a series of CTPB analogues showed that the selectivity of these compounds toward p300 and PCAF is dependent on the length of the C6-aliphatic chain and the presence of terminal polar groups.[38]

We recently reported a series of long-chain alkylidenemalonates (LoCAMs), which were inspired by the structural simplification of anacardic acid.[39] One of these compounds, diethyl pentadecylidenemalonate **1** (SPV106, Figure 3), has a unique activity profile. This compound exhibits inhibitory properties against KAT3A/3B (CBP/p300) with a potency comparable to that of anacardic acid, and it simultaneously enhances the acetylating activity of KAT2B. Therefore, it is the first mixed activator/inhibitor of protein acetyltransferases.[39]

As a result of its peculiar activity profile, derivative **1** was successfully used as a chemical probe[40] in a study that corre-

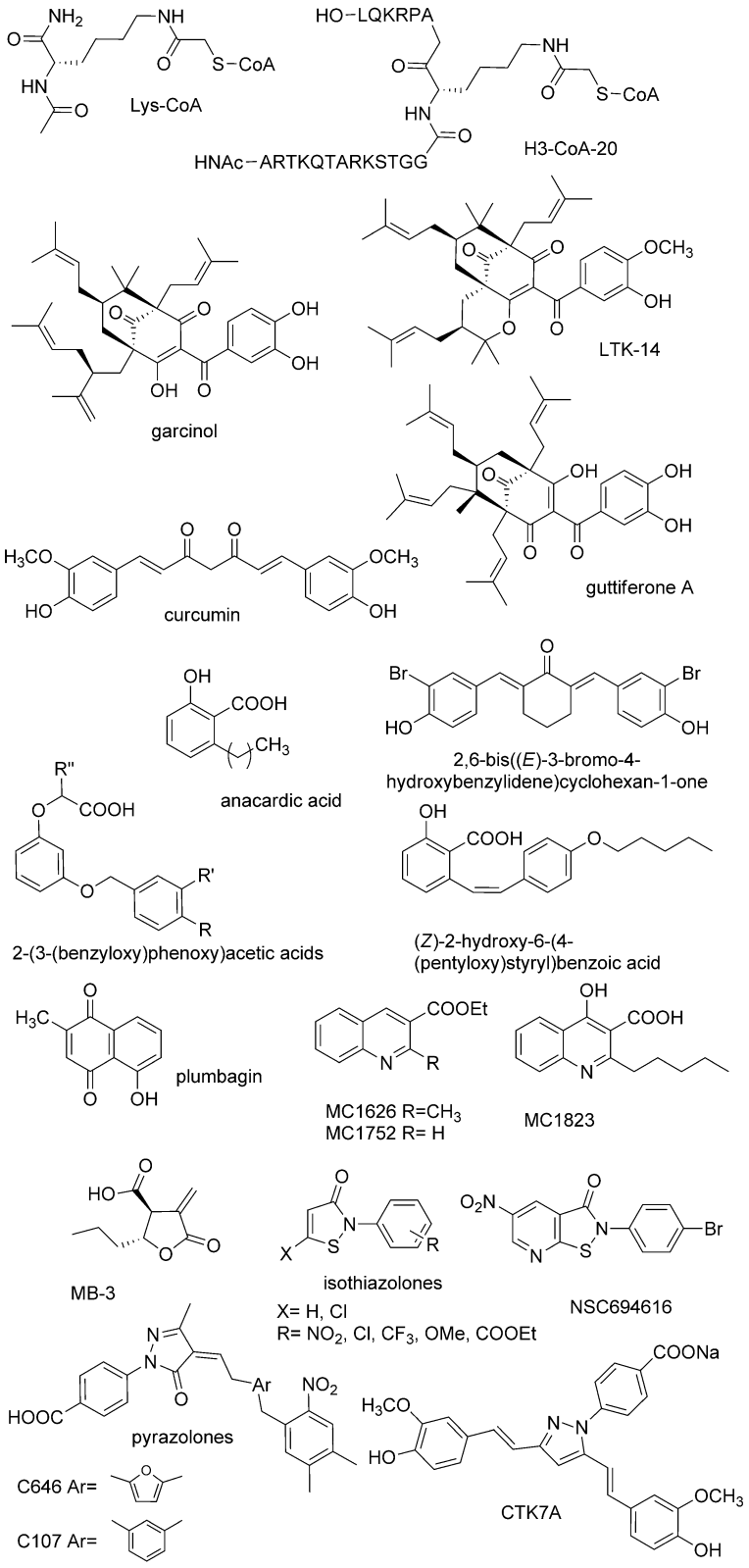

Figure 2. Different classes of KAT inhibitors.

lated Duchenne cardiomyopathy with KAT2B-mediated lysine acetylation levels of connexin 43.[22b] It was also examined during investigations of the role of KAT enzymes in the regulation of the extinction of conditioned fear and neuronal plasticity[23f] and the role of KAT2B acetyltransferase activity in the regulation of nitroglycerin-dependent arterial relaxation[22a] and wound healing.[41] More recently, treatment with compound **1** has been shown to reverse alterations in human cardiac mesenchymal cells obtained from diabetic patients and restore cellular function.[22c]

The uncommon biological properties of derivative **1** prompted us to explore the structure–activity relationships of LoCAMs. First, we focused on the alkyl chain and the flexibility of the scaffold.[39a] Similar to what was previously reported for MB-3[36] and CTPB analogues,[38] we found that variations in the alkyl chain length influenced the activity profile of KAT modulators, whereas all other modifications, such as variations in flexibility/rigidity of the core structure and the introduction of substituents, were detrimental.[39a] Indeed, not only the selectivity toward different KAT enzymes, but also the inhibitory and activating properties, varied depending on the substitution pattern.[39a]

As a further exploration of the structure–activity relationships of this class of KAT modulators, and with the aim of identifying potential structural features that differentially affect the activity of acetyltransferases, we herein describe the synthesis of a number of 1,3-dicarbonyl derivatives (Figure 4), formally derived by the replacement of one or both ester functions with keto- or carboxylic acid groups while keeping the alkyl chain length constant. In addition, because we previously found that the diketo analogue of compound **1** (derivative **2 d**, Figure 4) retained inhibitory activity against KAT3A,[39a] we also prepared a few shorter- and longer-chain homologues of **2 d**.

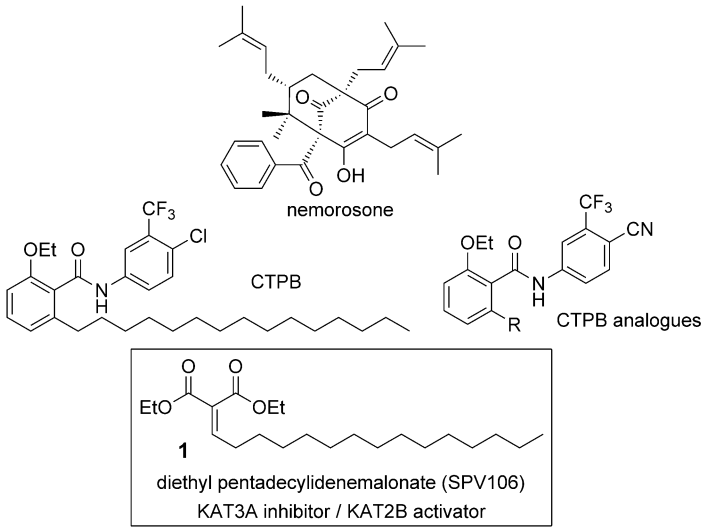

Figure 3. KAT activators.

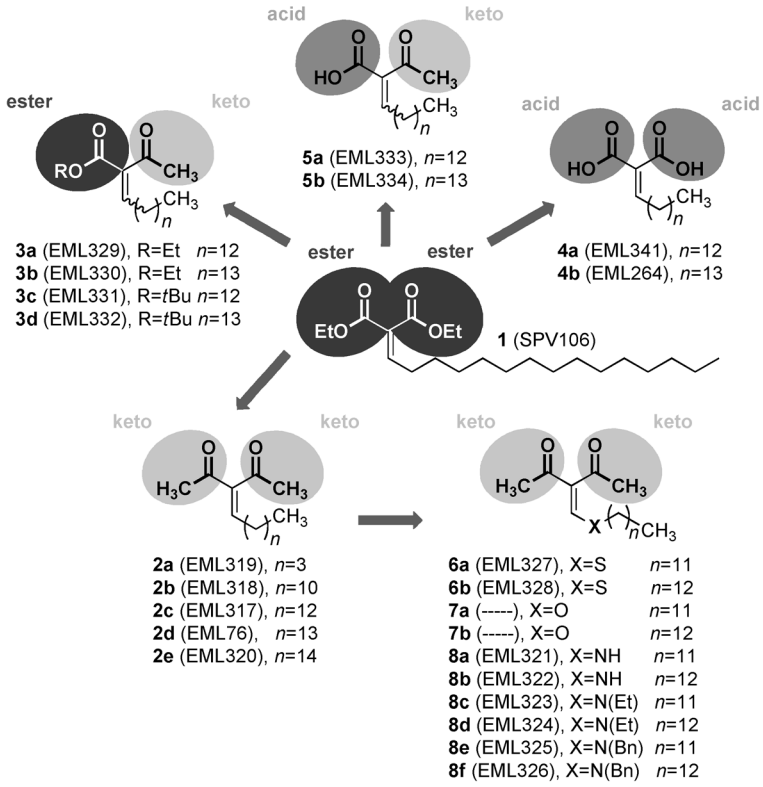

Figure 4. 1,3-Dicarbonyl derivatives **2a–e**, **3a–d**, **4a**,**b**, **5a**,**b**, **6a**,**b**, **7a**,**b**, and **8a–f**.

To avoid time-consuming, expensive assays, all compounds were preliminarily screened using a surface plasmon resonance-based binding assay, which we recently reported,[30,39a,42] to study the interactions between small molecules and epigenetic enzymes. The effects of selected derivatives on the catalytic activity of the KAT2B and KAT3B enzymes was then determined, and the biological effects on different cell lines were evaluated.

Results and Discussion

Chemistry

Novel alkylidene derivatives **2**–**5** were prepared in a straightforward manner (Scheme 1) by Knoevenagel condensation of a 1,3-dicarbonyl derivative with the appropriate alkyl aldehydes,[39a] which were commercially available or obtained from the corresponding alcohol by oxidation with 2,2,6,6-tetramethylpiperidine 1-oxyl (TEMPO), according to previously published procedures.[43] Derivatives **2a–e**,[44] **3a–d**,[45] and **4a**,**b** were prepared by reacting, respectively, pentane-2,4-dione, ethyl 3-oxobutanoate, *tert*-butyl 3-oxobutanoate, or malonic acid with the appropriate aldehyde in dichloromethane using piperidine and acetic acid as the catalysts (Scheme 1). The hydrolysis of *tert*-butyl esters **3c**,**d** with trifluoroacetic acid (TFA) yielded the corresponding 2-alkylidene-3-oxobutanoic acids **5a**,**b**.

Notably, the Knoevenagel condensation of ethyl 3-oxobutanoate and *tert*-butyl 3-oxobutanoate with alkyl aldehydes furnished derivatives **3a**,**b** and **3c**,**d**, respectively, as mixtures of *E* and *Z* isomers, which were successfully separated by silica gel chromatography. However, interconversion spontaneously occurred, even at low temperatures. For this reason, compounds **3a–d** and the corresponding acids **5a**,**b** were biologically evaluated as the *E*/*Z* mixtures. Copies of the NMR spectra of the separated isomers of **3d** are provided as representative examples in the Supporting Information.

Alkylthiomethylidenepentane-2,4-diones **6a**,**b** and alkylaminomethylidenepentane-2,4-diones **8a–f**[46] were obtained in high yield (Scheme 2) by reacting, respectively, the appropriate alkyl amine or alkyl thiol with 3-(ethoxymethylene)-2,4-pentanedione **9** in THF at reflux.[47] Alkyloxymethylene-2,4-pentanediones **7a**,**b** were obtained in good yield (calculated by NMR analysis of the crude reaction mixture) under the same conditions from the corresponding alkyl alcohols. Unfortunately, compounds **7a**,**b** were sensitive to nucleophiles, including negligible amounts of water. Therefore, any attempt to purify these derivatives by chromatography was unsuccessful. Moreover, because an aqueous medium is required for biological screening, we abandoned any further purification efforts.

SPR-based binding assays

The most sensitive histone acetyltransferase assays typically involve radioactivity. However, these methods tend to be costly, particularly those involving radiolabeled acetyl-CoA, and require special handling precautions and radioactive disposal. In contrast, non-radioactive spectrophotometric assays are rather quick, safe, and inexpensive, but they are plagued by signifi-

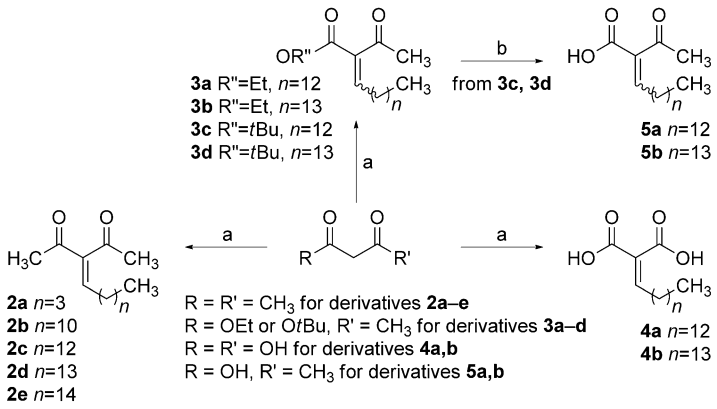

Scheme 1. *Reagents and conditions*: a) alkyl aldehyde, AcOH, piperidine, CH_2Cl_2, RT, 2–12 h; b) TFA/CH_2Cl_2 (5:95), RT, 30 min.

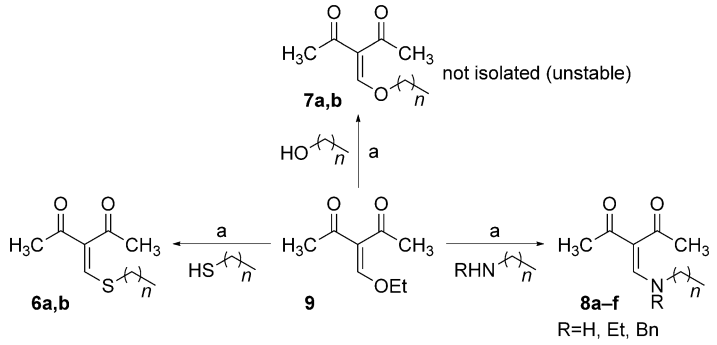

Scheme 2. *Reagents and conditions*: a) alkyl amine, thiol, or alcohol ($n = 11$, 12), THF, reflux, 2 h.

cantly lower sensitivity (enzyme-coupled assays), interference from compound spectral density, autofluorescence, and/or reaction of the enzyme-free sulfhydryl groups or substrates/products with common coumarin reporters.[48]

Surface plasmon resonance (SPR) biosensor-based assays are well suited to overcome many of the limitations of traditional assays and are increasingly important in medicinal chemistry for hit/lead identification and the optimization process.[49] Recently, we established an SPR-based binding assay and successfully employed it to study the real-time kinetic and thermodynamic parameters of ligand–protein interactions between small-molecule derivatives and KAT3B[39] as well as other epigenetic targets.[42]

Therefore, we used this assay to select compounds capable of binding to at least one of the acetyltransferase enzymes (KAT2B and/or KAT3B). Thus, the human recombinant KAT3B (aa 1284–1673) and KAT2B (aa 492–658) catalytic domains were immobilized (up to ~10000 response units (RU)) on different flow cells of the biosensor chip, and 1,3-dicarbonyl derivatives **2**–**8** were injected at various concentrations (from 25–100 μM) over the protein surface. To decrease false positives from detergent-sensitive, nonspecific aggregation-based binding, 0.005% NP20 was added to the running buffer in all experiments. In addition, to evaluate potential nonspecific binding, all compounds were injected on an immobilized myoglobin. The binding of each compound was read in real time as the change in mass at the sensor surface. After injection, running buffer was allowed to flow over the surface, and the dissociation of compounds from the surface was observed (Figure 5). Equilibrium dissociation constant (K_D) values were derived from the ratio between kinetic dissociation (k_d) and association (k_a) constants, obtained by fitting data from all injections at different concentrations of each compound using the simple 1:1 Langmuir binding fit model of the BIAevaluation software.

Tetradecylidene- and pentadecylidene-substituted pentane-2,4-diones, malonic acids, and 3-oxobutanoic acids (**2c**,**d**, **4a**,**b**, and **5a**,**b**, respectively) efficiently interacted with the immobilized proteins as demonstrated by the concentration-dependent responses and the clearly evident exponential curves during both the association and dissociation phases (the sensorgrams for compounds **2d**, **4b**, and **5b** are displayed in Figure 5). However, both 3-oxobutanoates **3a**–**d** and derivatives **6**–**8**, which are characterized by the presence of a heteroatom in their aliphatic chains, showed negligible interaction (not shown). In addition, in agreement with what we previously reported for LoCAMs,[39a] we found that variations in the alkyl chain length influenced the binding profile of the tested pentane-2,4-diones **2a**–**e**. In fact, superior (**2e**) and inferior (**2a**,**b**) homologues also produced good sensorgrams but showed low and/or concentration-independent responses (not shown).

Histone acetyltransferase IC_{50} profiling

After application of the SPR-based ligand filtering procedure, the effect of the selected derivatives (SPR+) **2c**,**d**, **4a**,**b**, and **5a**,**b** on the catalytic activity of the human recombinant acetyltransferase enzymes KAT3B and KAT2B was determined in HotSpot HAT activity assays, which were performed by Reaction Biology Corporation (Malvern, PA, USA) according to the company's standard operating procedure, using curcumin[28] and anacardic acid (AA),[26] respectively, as reference compounds. Two negative controls (SPR−, **6b** and **8b**) were also tested to cross-validate the selection method.

As shown in Table 1, all of the SPR+ derivatives substantially affected the activity of one or both of the HAT enzymes. In particular, pentane-2,4-diones **2c**,**d** induced a marked dose-dependent increase in the enzymatic activity of KAT2B (HAT activity at 100 μM: 229% and 389%, respectively; Table 1), while they did not affect the activity of KAT3B. In contrast, malonic acids **4a**,**b** strongly inhibited both enzymes, with IC_{50} values in the low micromolar range (1.3 and 1.1 μM, respectively, for KAT3B, and 50.3 and 21.1 μM, respectively, for KAT2B; Table 1 and Figure 6), which are similar to or more potent than the reference compounds (IC_{50}: 6.5 μM and 33.9 μM for curcumin and AA, respectively; see Table 1).

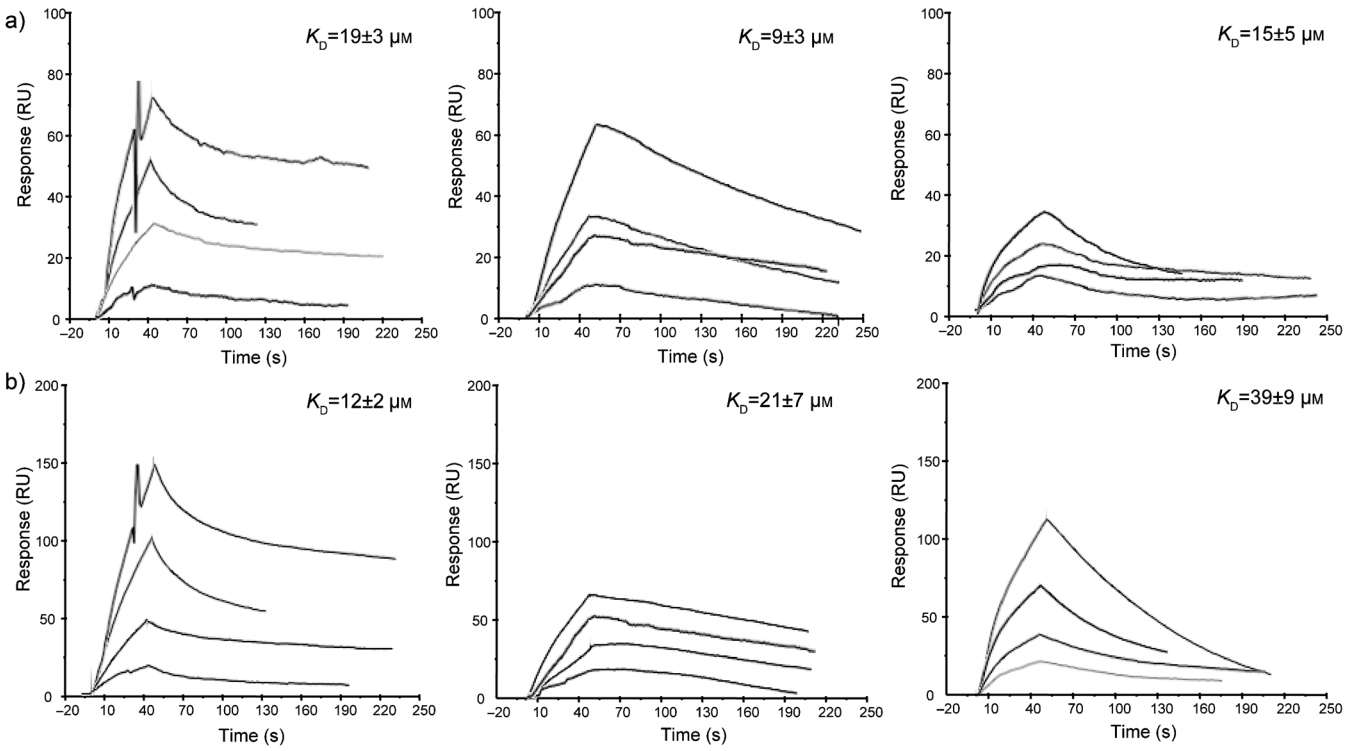

Figure 5. Sensorgrams obtained from SPR interaction analysis of compounds **2d** (left), **4b** (middle), and **5b** (right) binding to immobilized a) hKAT3B/p300 (catalytic domain, aa 1284–1673) and b) hKAT2B/PCAF (catalytic domain, aa 492–658). Each compound was injected at four different concentrations (25, 50, 75, and 100 μM). Equilibrium dissociation constants (K_D) were derived from the ratio between kinetic dissociation (k_d) and association (k_a) constants obtained by fitting data from all of the injections at various concentrations of each compound using the BIAevaluation software package (version 4.1) and the simple 1:1 Langmuir binding model.

Table 1. Effects of compounds **2c**,**d**, **4a**,**b**, **5a**,**b**, **6b**, and **8b** on the activity of KAT2B and KAT3B.[a]

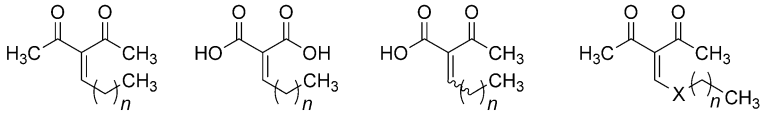

2c (EML317), *n*=12 **4a** (EML341), *n*=12 **5a** (EML333), *n*=12 **6b** (EML328), X=S *n*=12
2d (EML76), *n*=13 **4b** (EML264), *n*=13 **5b** (EML334), *n*=13 **8b** (EML322), X=NH *n*=12

Compd	IC_{50} [μM][b] or Activity [%][c,d] p300/KAT3B[e]	PCAF/KAT2B[e]
1	18.8±1.2%	137±5%
2c	NI[f]	229±7%
2d	NI[f]	389±9%
4a	1.3±0.1[b]	50.3±0.4[b]
4b	1.1±0.1[b]	21.1±0.5[b]
5a	2.4±0.1[b]	346±9%
5b	4.7±0.3[b]	497±12%
6b	NI[f]	NI[f]
8b	NI[f]	NI[f]
curcumin[g]	6.5±0.2[b]	NT[h]
AA[g]	NT[h]	33.9±0.7[b]

[a] Compounds were tested in 10-dose IC_{50} mode with threefold serial dilutions starting at 100 μM. [b] Data were analyzed with GraphPad Prism software (version 6.0) for IC_{50} curve fits. [c] Enzyme activity percentage determined at 100 μM with respect to DMSO. [d] Values are the means ± SD determined for at least two separate experiments and are indicated in percentage points. [e] Histone H3 was used as substrate (5 μM), and [acetyl-^{3}H]acetyl coenzyme A (3.08 μM) was used as an acetyl donor. [f] Negligible inhibition or activation. [g] Control compounds curcumin and anacardic acid were tested in a 10-dose IC_{50} mode with threefold serial dilutions starting at 100 μM. [h] Not tested.

Notably, 3-oxobutanoic acids **5a**,**b** efficiently inhibited KAT3B (IC_{50} values of 2.4 μM and 4.7 μM, respectively) but also caused strong amplification of KAT2B enzymatic activity in a dose-dependent manner (HAT activity at 100 μM: 346 and 497%, respectively; Table 1), and this effect was even more significant than that observed for pentane-2,4-diones **2c**,**d** (see above). In accordance with the SPR experiments, the negative controls negligibly affected the enzymatic activity of KAT2B and KAT3B (see **6b** and **8b** in Table 1).

Biological effects on various tumor cell lines

The aberrant regulation (or altered expression) of histone-modifying enzymes may differentially affect the level of histone modifications in different cells, and this may influence both normal biology and disease processes. Indeed, different histone modification (comprising acetylation) signatures have been recently described for a number of human cancer cell lines.[50] Therefore, we decided to examine the effects of tested compounds on three different cell lines, namely human leukemic monocyte lymphoma U937 cells and human cervical car-

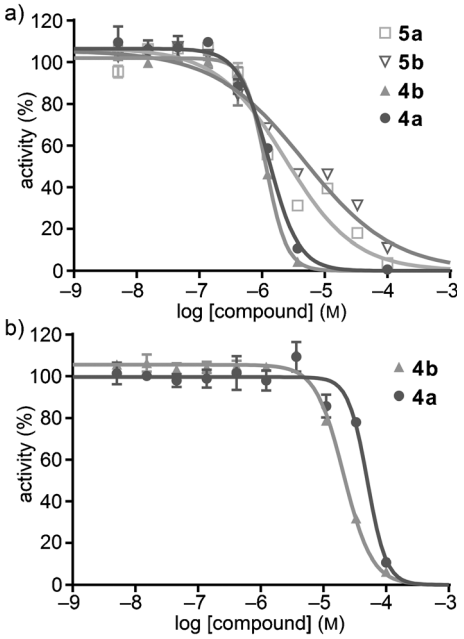

Figure 6. Dose–response inhibition of a) KAT3B/p300 and b) KAT2B/PCAF by compounds **4a**,**b** and **5a**,**b**. Compounds were tested in 10-dose IC_{50} mode with threefold serial dilutions starting at 100 μM. Data were analyzed with GraphPad Prism software (version 6.0) for curve fits using a sigmoidal dose–response with a variable slope equation.

cinoma C33A and HeLa cells. First, an MTT assay was performed after treatment with SPR+ derivatives to assess the maximum concentration of compounds that could be used without significantly affecting cell viability. For solid C33A and HeLa tumor cell lines, we observed no significant decrease in the number of metabolically active cells after 24 h of treatment with concentrations up to 200 μM for derivatives **2c**,**d** and **4a**,**b** and up to 50 μM for compounds **5a**,**b** (data not shown). On the other hand, in the case of the more sensitive U937 cell line (Figure 7a), we registered a significant decrease in cell viability starting from lower concentrations of tested compounds (100 μM for **2c**,**d** and **4a**,**b** and 10 μM for **5a**,**b**, respectively).

All of the SPR+ derivatives were then screened for their effects on the cell cycle using the U937 cell line. After 24 h of treatment, compounds **4b**, **5a**, and **5b** were able to arrest the cell cycle in the G_1 phase (Figure 7b). In the case of the latter two compounds, this occurred at concentrations as low as 10 μM and induced an increase in the number of sub-G_1 hypodiploid nuclei, as detected by the Nicoletti method (Figure S1, Supporting Information).[51] This result is consistent with the importance of acetylation for control of the G_1/S transition.[19i,52] Under the same conditions, the other derivatives had no significant effects on the cell cycle.

We then examined the effects of compounds **2d**, **4b**, and **5b** on the acetylation levels of specific lysine residues of core histones H3 (K9) and H4 (K5) in the three cell lines. The effect on the overall level of H4 acetylation was also observed. Cells were incubated for 24 h with vehicle and tested with compounds at the indicated concentrations or the reference compound suberoylanilide hydroxamic acid (SAHA; 5 μM),[16] and the histone extracts were then immunoblotted with antibodies to specific histone acetylation sites (Figure 8). Consistent with the different patterns of acetylation recently described by Garcia and co-workers,[50] we observed that the tested compounds differentially affected the global H4 acetylation level (Figure S2, Supporting Information) as well as the H4K5ac[53] and H3K9ac levels in the three cell lines. In fact, the effect of pentane-2,4-dione **2d** on both markers was negligible in U937 cells (Figure 8, row c, left and middle panels), whereas a decrease was observed in both cervical carcinoma cell lines, which was more evident for H4K5ac (Figure 8, rows a and b). Both malonic acid **4b** and 3-oxobutanoic acid **5b** induced a marked decrease in the acetylation of lysine H4K5 in C33A cells (Figure 8, row a, left panel), whereas no appreciable effect on the same marker was detected in HeLa cells, and an increase was observed in U937 cells (Figure 8, rows b and c, respectively).

In contrast, derivative **4b** induced a moderate decrease in the acetylation of H3K9 in C33A and HeLa cells (Figure 8, rows a and a, respectively, middle panels), and there was no appreciable variation in U937 cells (Figure 8, row c, middle panel), whereas **5b** induced a decrease in the acetylation of H3K9 in C33A and HeLa cells (Figure 8, rows a and b, respectively, middle panels) and a marked increase in the acetylation level in U937 cells (Figure 8, row c, middle panel). As expected, treatment with the reference compound SAHA reliably showed a significant increase in the lysine acetylation level (Figure 8).

Conclusions

Lysine acetylation is a reversible process, resulting from the opposing actions of the KDAC and KAT enzymes, which is crucial for the regulation of a number of cellular functions, including chromatin remodeling, gene expression, cytoskeleton dynamics, energy metabolism, endocytosis, autophagy, and even signaling from the plasma membrane. Dysregulation of the activity of KAT enzymes has been related to a variety of diseases and/or pathological cellular states including cancer, inflammation, viral diseases, cardiomyopathies, and disturbances in neuronal cell plasticity and differentiation, yet their role is still unclear. Therefore, the development of selective modulators of these enzymes is of paramount importance, because such molecules could be invaluable tools for assessing the implication of KATs in several pathologies.

We recently identified diethyl pentadecylidenemalonate (**1**; SPV106) as having a previously unobserved activity profile against protein acetyltransferases (i.e., the ability to inhibit the activity of KAT3A/3B and simultaneously enhance that of KAT2B).[39] Because of this unusual activity profile, an SPV106 derivative was successfully used as a chemical probe to study the role of KAT enzymes in cardiovascular, neurological, physiological, and/or pathological pathways.[22,23f,41] With the aim of further investigating structure–activity relationships, we prepared a number of 1,3-dicarbonyl derivatives as analogues of SPV106, replacing one or both of the ester functions with keto- or carboxylic acid groups. Taking advantage of a binding assay recently established by our group,[30,39a,42] we applied

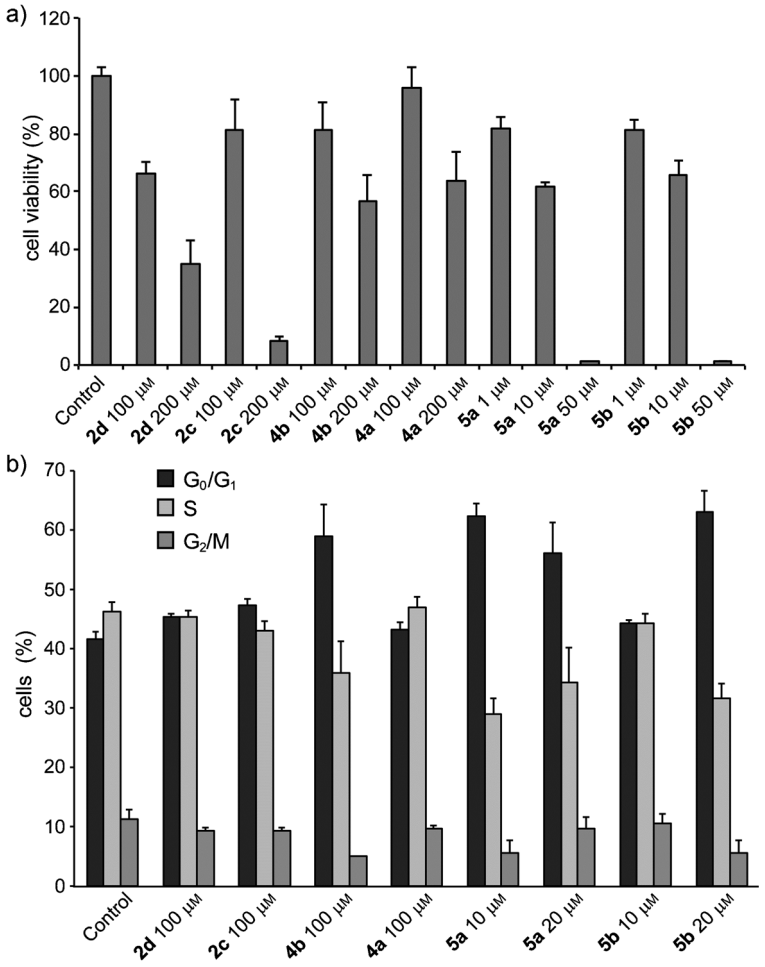

Figure 7. Cell viability and cell-cycle analysis in U937 cells by fluorescence-activated cell sorting (FACS). a) Cell viability was assessed by measuring the mitochondrial-dependent reduction of MTT to formazan. b) U937 cells were treated with compounds **2c**,**d**, **4a**,**b**, and **5a**,**b** at the indicated concentrations for 24 h, stained with propidium iodide, and subjected to flow cytometric analysis to determine the distribution of cells in each phase of the cell cycle. Data are reported as the mean ± SD of at least three independent experiments. Statistical significance (relative to controls, Student's *t* test): a) $p < 0.05$ for **5a** and **5b** at 1 μM and for **4a** at 100 μM, $p < 0.005$ for all other compounds and concentrations; b) $p < 0.005$ (G_1 phase of cells treated with **4b**, **5a**, and **5b**).

a SPR-based ligand filtering procedure to select compounds capable of binding to the acetyltransferase enzymes KAT2B and KAT3B. We found that the presence of a heteroatom in the aliphatic chain of tested molecules resulted in negligible interactions and that, similar to what was previously reported for LoCAMs[39a] by us and other groups for analogues of MB-3[36] and CTPB,[38] variations in the length of the alkyl chain greatly influenced the binding profile of the tested derivatives; tetradecylidene- and pentadecylidene-substituted compounds interacted efficiently with both of the immobilized proteins, whereas superior and inferior homologues had low and/or concentration-independent responses. When tested in a biochemical assay, all of the selected derivatives (SPR+) markedly affected the catalytic activity of one or both of the KAT enzymes, and this effect was related to the nature of the carbonyl functions of the molecules. In fact, pentane-2,4-diones **2c**,**d** induced a marked and concentration-dependent increase in the enzymatic activity of KAT2B and did not affect the activity of KAT3B; malonic acids **4a**,**b** strongly inhibited both enzymes with IC_{50} values in the low micromolar range, and 3-oxobutanoic acids **5a**,**b** efficiently inhibited KAT3B but also caused strong amplification of the KAT2B enzymatic activity in a dose-dependent manner. Under the same conditions, SPR-negative controls negligibly affected the enzymatic activity of KAT2B and KAT3B. We then decided to evaluate the effects of derivatives **2d**, **4b**, and **5b** on the acetylation of lysine residues H4K5 and H3K9 in C33A, HeLa, and U937 cell lines. Consistent with the distinct patterns of acetylation (and other histone modifications) in the various cancer cell lines,[50] we observed differential modulation of the same lysine marker induced by the compounds in the different cell lines. This observation is not surprising, considering that in the cellular context, acetyltransferases are similar to other enzymes by not being isolated; they participate in complex pathways and actively cross-talk with each other and with other proteins. In particular, we found that malonic acid **4b** and 3-oxobutanoic acid **5b** induce a marked decrease in H4K5ac in C33A cells, whereas a significant increase in H3K9ac was detected in U937 cells after treatment with 3-oxobutanoic acid **5b**.

The differences observed in the activity profile of the structurally related compounds **2c**,**d**, **4a**,**b**, and **5a**,**b** against the two acetyltransferases could have a number of explanations, and the mechanisms underlying their biological effects remain unclear. However, it has been previously reported that small modifications in structurally related compounds lead to dramatic differences in terms of selectivity between KAT2B and KAT3B.[20c] Moreover, is worth mentioning that the catalytic mechanisms of the two enzymes are different, with KAT2B using a ternary complex mechanism,[54] and a Theorell–Chance "hit and run" model proposed for KAT3B[55] in which the histone peptide binds weakly to the enzyme–cofactor complex, allowing enough time for the lysine side chain to snake through the enzyme tunnel and receive the acetyl group.[56] Furthermore, it has been recently reported that displacement of the flexible auto-inhibitory loop (AIL) and inhibitory RING domain enhance the activity of KAT3A/3B enzymes,[57] whereas another report suggested that KAT2B is a dimer in its functional ATAC complex.[58] Ongoing experiments will shed more light on this issue.

In conclusion, in this study, we obtained different activity profiles against KAT2B and KAT3B (pure KAT2B activator, pan-inhibitor, or mixed KAT2B activator/KAT3B inhibitor) by manipulating the carbonyl functions of a series of analogues of SPV106. Enzyme activators are rarely pursued in chemical biology and drug discovery efforts, but they may be invaluable reagents alone or in combination with inhibitors.[42] Therefore, a few of the compounds described, namely derivatives **2c**,**d** (EML317, EML76), **4a**,**b** (EML341, EML264), and **5a**,**b** (EML333,

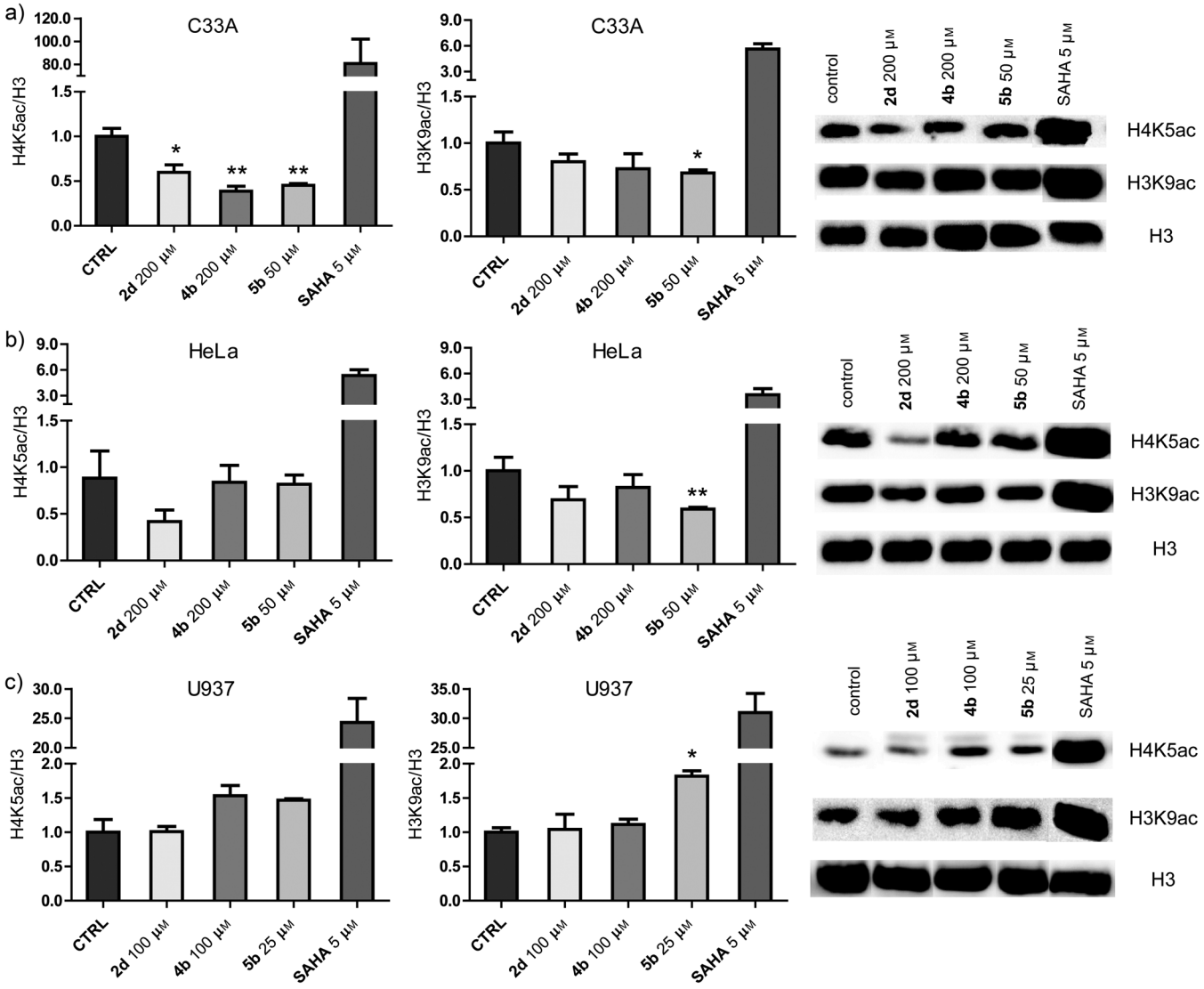

Figure 8. Western blot analyses performed with compounds **2d**, **4b**, and **5b** at the indicated concentrations for 24 h on the acetylation of the specific lysine residues H4K5 (left column) and H3K9 (middle column) in histone extracts from a) C33A and b) HeLa carcinoma cells, and c) U937 leukemic monocyte lymphoma cells. Acetylation was detected by immunoblotting with antibodies specific for histone acetylation sites as indicated. Total histone H3 was used to check for equal loading. SAHA (5 μM) was used as a reference compound. Signals were detected with the ImageQuant LAS 4000 digital imaging system (GE Healthcare, Waukesha, WI, USA) and quantified by ImageQuantTL software (version 8.1); total histone H3 levels were used for normalization. The results are reported as the mean ± SD of three independent experiments with the control data set to 1; statistical significance: $*p<0.05$, $**p<0.01$, $***p<0.001$ relative to controls (Student's *t* test).

EML334), may be useful chemical tools for mechanistic studies of lysine acetylation and its implications in physiological and/or pathological processes.

Experimental Section

Chemistry

General directions: All chemicals were purchased from Aldrich Chimica (Milan, Italy) and were of the highest purity. All solvents were reagent grade and were purified and dried by standard methods when necessary. All reactions requiring anhydrous conditions were conducted under a positive atmosphere of nitrogen in oven-dried glassware. Standard syringe techniques were used for the anhydrous addition of liquids. Reactions were routinely monitored by TLC performed on aluminum-backed silica gel plates (Merck DC, Alufolien Kieselgel 60 F254) with spots visualized by UV light ($\lambda =$ 254, 365 nm) or using a $KMnO_4$ alkaline solution. Solvents were removed using a rotary evaporator operating at a reduced pressure of ≈10 Torr. Organic solutions were dried over anhydrous Na_2SO_4. Chromatographic separations were performed on silica gel (silica gel 60, 0.015–0.040 mm; Merck DC) columns. Melting points were determined on a Stuart SMP30 melting point apparatus in open capillary tubes and were uncorrected. Infrared (IR) spectra were recorded neat with a Shimadzu IR Affinity-1 FTIR fitted with a MIRacle 10 single reflection ATR accessory at room temperature. ^1H and ^{13}C NMR spectra were recorded at 300 MHz and 75 MHz, respectively, with a Bruker Avance 300 spectrometer. Chemical shifts are reported in δ (ppm) relative to the internal reference tetramethylsilane (TMS). Mass spectra were recorded with a Finnigan LCQ DECA TermoQuest (San Jose, USA) mass spectrometer in electrospray-

positive and -negative ionization modes (ESI-MS). The purity of the test compounds was established by combustion analysis, confirming purity $\geq$95%. Elemental analyses (C, H, N) were performed with a PerkinElmer 2400 CHN elemental analyzer, and the analytical results were within $\pm$0.4% of the theoretical values (Table S1, Supporting Information).

General procedure for the synthesis of derivatives 2a–d: A stirred solution of the appropriate alkyl aldehyde (4.00 mmol) and 2,4-pentanedione (acetylacetone) (4.40 mmol) in anhydrous methylene chloride (3 mL) was treated with piperidine (0.08 mmol) and acetic acid (0.08 mmol) at 0 °C. The reaction mixture was stirred at room temperature for 1 h (TLC monitoring), diluted with methylene chloride (50 mL), washed with brine (3×10 mL), and dried (Na_2SO_4). After removing the solvent, the crude residue was purified by column chromatography on silica gel (*n*-hexane/EtOAc) to afford the title compounds.

3-Pentylidenepentane-2,4-dione (2a, EML319): Colorless oil (619 mg, 92%): ^{1}H NMR (300 MHz, $CDCl_3$): δ=6.67 (t, J=7.7 Hz, 1H), 2.30 (s, 6H), 2.28–2.15 (m, 2H), 1.52–1.42 (m, 2H), 1.41–1.31 (m, 2H), 0.92 ppm (t, J=7.1 Hz, 3H); ^{13}C NMR (75 MHz, $CDCl_3$): δ= 203.5, 197.2, 146.9, 145.4, 30.9, 29.5, 26.1, 22.5, 13.9 ppm; IR (neat): $\tilde{\nu}$=2959, 2932, 2862, 1705, 1667, 1628 cm^{-1}; ESI-MS *m/z*: 169 $[M+H]^+$; Anal. calcd for $C_{10}H_{16}O_2$: C 71.39, H 9.59, found: C 71.54, H 9.61.

3-Dodecylidenepentane-2,4-dione (2b, EML318): Colorless oil (991 mg, 93%): ^{1}H NMR (300 MHz, $CDCl_3$): δ=6.71 (t, J=7.7 Hz, 1H), 2.35 (s, 6H), 2.28–2.18 (m, 2H), 1.53–1.42 (m, 2H), 1.34–1.22 (m, 16H), 0.89 ppm (t, J=6.5 Hz, 3H); IR (neat): $\tilde{\nu}$=2955, 2924, 2855, 1705, 1667, 1628 cm^{-1}; ESI-MS *m/z*: 267 $[M+H]^+$; Anal. calcd for $C_{17}H_{30}O_2$: C 76.64, H 11.35, found: C 76.83, H 11.38.

3-Tetradecylidenepentane-2,4-dione (2c, EML317): Colorless oil (1095 mg, 93%): ^{1}H NMR (300 MHz, $CDCl_3$): δ=6.66 (t, J=7.7 Hz, 1H), 2.27 (s, 6H), 2.25–2.13 (m, 2H), 1.51–1.40 (m, 2H), 1.28–1.16 (m, 20H), 0.86 ppm (t, J=6.5 Hz, 3H); IR (neat): $\tilde{\nu}$=2924, 2855, 1713, 1670, 1624 cm^{-1}; ESI-MS *m/z*: 295 $[M+H]^+$; Anal. calcd for $C_{19}H_{34}O_2$: C 77.50, H 11.64, found: C 77.69, H 11.67.

3-Pentadecylidenepentane-2,4-dione (2d, EML76):[39a] Colorless oil (1098 mg, 89%): ^{1}H NMR (300 MHz, $CDCl_3$): δ=6.70 (t, J=7.7 Hz, 1H), 2.34 (s, 6H), 2.28–2.19 (m, 2H), 1.54–1.48 (m, 2H), 1.38–1.26 (m, 22H), 0.99 ppm (t, J=6.3 Hz, 3H); ^{13}C NMR (75 MHz, $CDCl_3$): δ= 203.7, 197.2, 147.1, 145.3, 32.1, 31.8, 29.8, 29.6, 29.5, 28.8, 26.2, 26.2, 22.8, 14.3 ppm; IR (neat): $\tilde{\nu}$=2916, 2851, 1701, 1664, 1636 cm^{-1}; ESI-MS *m/z*: 309 $[M+H]^+$; Anal. calcd for $C_{20}H_{36}O_2$: C 77.87, H 11.76, found: C 78.05, H 11.79.

3-Hexadecylidenepentane-2,4-dione (2e, EML320): Colorless oil (1238 mg, 96%): ^{1}H NMR (300 MHz, $CDCl_3$): δ=6.66 (t, J=7.7 Hz, 1H), 2.28 (s, 6H), 2.26–2.16 (m, 2H), 1.53–1.43 (m, 2H), 1.30–1.23 (m, 24H), 0.86 ppm (t, J=6.3 Hz, 3H); IR (neat): $\tilde{\nu}$=2916, 2851, 1701, 1663, 1636 cm^{-1}; ESI-MS *m/z*: 323 $[M+H]^+$; Anal. calcd for $C_{21}H_{38}O_2$: C 78.20, H 11.88, found: C 78.41, H 11.91.

General procedure for the synthesis of derivatives 3a–d: Derivatives **3a–d** were prepared by reacting the appropriate alkyl aldehyde and ethyl 3-oxobutanoate (for compounds **3a**,**b**) or *tert*-butyl 3-oxobutanoate (for compounds **3c**,**d**), according to the procedure used for derivatives **2a–e**. The crude residue was purified by column chromatography on silica gel (*n*-hexane/EtOAc) to afford the title compounds as a mixture of *E* and *Z* isomers.

Ethyl 2-acetylhexadec-2-enoate (3a, EML329):[45] Low-melting-point white solid (934 mg, 72%): 1:1 mixture of geometric isomers **a** and **b**; ^{1}H NMR (300 MHz, $CDCl_3$): δ=6.92 (t, J=7.7 Hz, 1H, isomer **a**), 6.85 (t, J=7.7 Hz, 1H, isomer **b**), 4.31 (q, J=7.1 Hz, 2H, isomer **b**), 4.25 (q, J=7.1 Hz, 2H, isomer **a**), 2.36–2.27 (m, 5H, isomer **b** and 3H, isomer **a**), 2.25–2.21 (m, 2H, isomer **a**), 1.55–1.40 (m, 2H, isomer **a** and 2H isomer **b**), 1.30–1.21 (m, 23H, isomer **a** and 23H isomer **b**), 0.88 ppm (br t, J=6.3 Hz, 3H, isomer **a** and 3H, isomer **b**); IR (neat): $\tilde{\nu}$=2922, 2853, 1728, 1701, 1638, 1622 cm^{-1}; ESI-MS *m/z*: 325 $[M+H]^+$; Anal. calcd for $C_{20}H_{36}O_3$: C 74.03, H 11.18, found: C 73.92, H 11.20.

Ethyl 2-acetylheptadec-2-enoate (3b, EML330): Low-melting-point white solid (1056 mg, 78%): 1:1 mixture of geometric isomers **a** and **b**; ^{1}H NMR (300 MHz, $CDCl_3$): δ=6.91 (t, J=7.7 Hz, 1H, isomer **a**), 6.83 (t, J=7.7 Hz, 1H, isomer **b**), 4.29 (q, J=7.1 Hz, 2H, isomer **b**), 4.23 (q, J=7.1 Hz, 2H, isomer **a**), 2.36–2.27 (m, 5H, isomer **b** and 3H, isomer **a**), 2.27–2.18 (m, 2H, isomer **a**), 1.54–1.40 (m, 2H, isomer **a** and 2H isomer **b**), 1.34–1.16 (m, 25H, isomer **a** and 25H isomer **b**), 0.86 ppm (br t, J=6.3 Hz, 3H, isomer **a** and 3H, isomer **b**); ^{13}C NMR (75 MHz, $CDCl_3$): δ=201.2, 195.2, 166.7, 164.8, 149.2, 148.8, 137.7, 137.2, 61.3, 32.0, 30.1, 29.8, 29.6, 29.5, 28.7, 28.5, 27.0, 22.8, 14.3, 14.2 ppm; IR (neat): $\tilde{\nu}$=2913, 2851, 1717, 1670, 1643 cm^{-1}; ESI-MS *m/z*: 339 $[M+H]^+$; Anal. calcd for $C_{21}H_{38}O_3$: C 74.51, H 11.31, found: C 74.37, H 11.33.

***tert*-Butyl 2-acetylhexadec-2-enoate (3c, EML331)**: Low-melting-point white solid (1072 mg, 76%): 1:1 mixture of geometric isomers **a** and **b**; ^{1}H NMR (300 MHz, $CDCl_3$): δ=6.80 (t, J=7.9 Hz, 1H, isomer **a**), 6.75 (t, J=7.8 Hz, 1H, isomer **b**), 2.33–2.27 (m, 5H, isomer **b** and 3H, isomer **a**), 2.25–2.14 (m, 2H, isomer **a**), 1.55–1.40 (m, 11H, isomer **a** and 11H isomer **b**), 1.30–1.21 (m, 20H, isomer **a** and 20H isomer **b**), 0.88 ppm (br t, J=6.5 Hz, 3H, isomer **a** and 3H, isomer **b**); IR (neat): $\tilde{\nu}$=2924, 2855, 1724, 1701, 1636, 1620 cm^{-1}; ESI-MS *m/z*: 375 $[M+Na]^+$; Anal. calcd for $C_{22}H_{40}O_3$: C 74.95, H 11.44, found: C 74.79, H 11.43.

***tert*-Butyl 2-acetylheptadec-2-enoate (3d, EML332)**: Low-melting-point white solid (1056 mg, 72%): 1:1 mixture of geometric isomers **a** and **b**; ^{1}H NMR (300 MHz, $CDCl_3$): δ=6.80 (t, J=7.9 Hz, 1H, isomer **a**), 6.75 (t, J=7.8 Hz, 1H, isomer **b**), 2.33–2.27 (m, 5H, isomer **b** and 3H, isomer **a**), 2.25–2.14 (m, 2H, isomer **a**), 1.55–1.40 (m, 11H, isomer **a** and 11H isomer **b**), 1.30–1.21 (m, 22H, isomer **a** and 22H isomer **b**), 0.88 ppm (br t, J=6.5 Hz, 3H, isomer **a** and 3H, isomer **b**); IR (neat): $\tilde{\nu}$=2913, 2851, 1717, 1686, 1620 cm^{-1}; ESI-MS *m/z*: 389 $[M+Na]^+$; Anal. calcd for $C_{23}H_{42}O_3$: C 75.36, H 11.55, found: C 75.21, H 11.54.

General procedure for the synthesis of derivatives 4a–b: Derivatives **4a–b** were prepared by reacting the appropriate alkyl aldehyde and malonic acid according to the procedure used for derivatives **2a–e**. The crude residue was purified by column chromatography on silica gel (CH_2Cl_2/MeOH) to afford the title compounds.

2-Tetradecylidenemalonic acid (4a, EML341): White solid (991 mg, 83%): mp: 69–70 °C; ^{1}H NMR (300 MHz, [D$_6$]DMSO): δ= 6.99 (t, J=7.5 Hz, 1H), 2.42–2.29 (m, 2H), 1.44–1.33 (m, 2H), 1.32–1.15 (m, 20H), 0.85 ppm (t, J=6.2 Hz, 3H); IR (neat): $\tilde{\nu}$=2953, 2918, 2851, 1735, 1720, 1697, 1568 cm^{-1}; ESI-MS *m/z*: 297 $[M-H]^-$; Anal. calcd for $C_{17}H_{30}O_4$: C 68.42, H 10.13, found: C 68.27, H 10.15.

2-Pentadecylidenemalonic acid (4b, EML264): White solid (975 mg, 78%): mp: 73–75 °C; ^{1}H NMR (300 MHz, [D$_6$]DMSO): δ= 6.88 (t, J=7.6 Hz, 1H), 2.41–2.27 (m, 2H), 1.49–1.38 (m, 2H), 1.34–1.14 (m, 22H), 0.85 ppm (t, J=6.3 Hz, 3H); ^{13}C NMR (75 MHz, DMSO): δ=169.8, 167.1, 147.3, 129.8, 31.3, 29.1, 28.8, 22.1, 13.8 ppm; IR (neat): $\tilde{\nu}$=2954, 2916, 2848, 1735, 1710, 1697,

1568 cm^{-1}; ESI-MS *m/z*: 311 $[M-H]^-$; Anal. calcd for $C_{18}H_{32}O_4$: C 69.19, H 10.32, found: C 69.05, H 10.34.

General procedure for the synthesis of derivatives 5a–b: A mixture of TFA and CH_2Cl_2 (1:3, 12 mL) was added to ester derivatives **3c** or **3d** (1.00 mmol). The reaction was stirred at room temperature for 30 min and then concentrated in vacuo to give the title compounds as a mixture of *E* and *Z* isomers.

2-Acetylhexadec-2-enoic acid (5a, EML333): Low-melting-point white solid (284 mg, 96%): 2:1 mixture of geometric isomers **a** and **b**; ^1H NMR (300 MHz, $CDCl_3$): $\delta = 10.90$ (br s, 1H, isomer **a** and 1H isomer **b**), 7.41 (t, $J = 7.2$ Hz, 1H, isomer **a**), 7.16 (t, $J = 7.8$ Hz, 1H, isomer **b**), 2.88–2.78 (m, 2H, isomer **a**), 2.46 (s, 3H, isomer **a**), 2.40 (s, 3H, isomer **b**), 2.35–2.25 (m, 2H, isomer **b**), 1.62–1.40 (m, 2H, isomer **a** and 2H isomer **b**), 1.30–1.21 (m, 20H, isomer **a** and 20H isomer **b**), 0.88 ppm (br t, $J = 6.3$ Hz, 3H, isomer **a** and 3H, isomer **b**); IR (neat): $\tilde{\nu} = 2916$, 2851, 1713, 1682, 1624 cm^{-1}; ESI-MS *m/z*: 297 $[M+H]^+$; Anal. calcd for $C_{18}H_{32}O_3$: C 72.93, H 10.88, found: C 72.80, H 10.90.

2-Acetylheptadec-2-enoic acid (5b, EML334): Low-melting-point white solid (292 mg, 94%): 2:1 mixture of geometric isomers **a** and **b**; ^1H NMR (300 MHz, $CDCl_3$): $\delta = 10.90$ (br s, 1H, isomer **a** and 1H isomer **b**), 7.53 (t, $J = 7.1$ Hz, 1H, isomer **a**), 7.38 (t, $J = 7.7$ Hz, 1H, isomer **b**), 3.00–2.91 (m, 2H, isomer **a**), 2.50 (s, 3H, isomer **a**), 2.46 (s, 3H, isomer **b**), 2.45–2.35 (m, 2H, isomer **b**), 1.65–1.47 (m, 2H, isomer **a** and 2H isomer **b**), 1.40–1.15 (m, 22H, isomer **a** and 22H isomer **b**), 0.88 ppm (br t, $J = 6.4$ Hz, 3H, isomer **a** and 3H, isomer **b**); ^{13}C NMR (75 MHz, $CDCl_3$): $\delta = 201.9$, 201.1, 169.0, 165.5, 164.0, 153.7, 134.4, 131.0, 32.0, 31.4, 31.3, 30.0, 29.8, 29.6, 29.5, 28.7, 26.7, 22.8, 14.2 ppm; IR (neat): $\tilde{\nu} = 2922$, 2853, 1717, 1684, 1636 cm^{-1}; ESI-MS *m/z*: 311 $[M+H]^+$; Anal. calcd for $C_{19}H_{34}O_3$: C 73.50, H 11.04, found: C 73.35, H 11.06.

General procedure for the synthesis of derivatives 6a,b and 8a–f: To a solution of 3-(ethoxymethylene)-2,4-pentanedione **9**[47] (1.00 mmol) in anhydrous THF (3 mL), the appropriate alkylamine (1.00 mmol) or alkylthiol (2.00 mmol) was added, and the reaction mixture was stirred at reflux for 2 h (monitored by TLC). After cooling at room temperature, the solvent was removed, and the crude residue was purified by column chromatography on silica gel (CH_2Cl_2/EtOAc) to afford the title compounds.

Dodecanethiol, dodecanamine, and tridecanamine used for the preparation of derivatives **6a**, **8a**, and **8b**, respectively, were commercially available. Tridecanethiol used for the synthesis of **6b** and *N*-ethyldodecan-1-amine, *N*-ethyltridecan-1-amine, *N*-benzyldodecan-1-amine, and *N*-benzyltridecan-1-amine used for the synthesis of derivatives **8c**, **8d**, **8e**, **8f**, respectively, were prepared by standard synthetic procedures (see Supporting Information for details).

3-(Dodecylthiomethylene)pentane-2,4-dione (6a, EML327): Low-melting-point white solid (288 mg, 92%): ^1H NMR (300 MHz, $CDCl_3$): $\delta = 8.17$ (s, 1H), 2.83 (t, $J = 7.4$ Hz, 2H), 2.47 (s, 3H), 2.38 (s, 3H), 1.79–1.63 (m, 2H), 1.48–1.37 (m, 2H), 1.34–1.16 (m, 16H), 0.88 ppm (t, $J = 6.5$ Hz, 3H); IR (neat): $\tilde{\nu} = 2951$, 2920, 2847, 1659, 1643 cm^{-1}; ESI-MS *m/z*: 313 $[M+H]^+$; Anal. calcd for $C_{18}H_{32}O_2S$: C 69.18, H 10.32, S 10.26, found: C 69.32, H 10.34, S 10.27.

3-(Tridecylthiomethylene)pentane-2,4-dione (6b, EML328): Low-melting-point white solid (307 mg, 94%): ^1H NMR (300 MHz, $CDCl_3$): $\delta = 8.16$ (s, 1H), 2.83 (t, $J = 7.4$ Hz, 2H), 2.47 (s, 3H), 2.38 (s, 3H), 1.78–1.65 (m, 2H), 1.48–1.37 (m, 2H), 1.33–1.19 (m, 18H), 0.88 ppm (t, $J = 6.5$ Hz, 3H); ^{13}C NMR (75 MHz, $CDCl_3$): $\delta = 197.7$, 194.7, 162.6, 134.2, 38.3, 32.1, 31.1, 30.2, 29.8, 29.6, 29.3, 28.6, 27.8, 22.8, 14.2 ppm; IR (neat): $\tilde{\nu} = 2951$, 2917, 2847, 1659, 1643 cm^{-1}; ESI-MS *m/z*: 327 $[M+H]^+$; Anal. calcd for $C_{19}H_{34}O_2S$: C 69.89, H 10.50, S 9.82, found: C 70.05, H 10.52, S 9.84.

3-((Dodecylamino)methylene)pentane-2,4-dione (8a, EML321):[46] Low-melting-point pale-yellow solid (287 mg, 97%): ^1H NMR (300 MHz, $CDCl_3$): $\delta = 11.07$ (br s, 1H), 7.71 (d, $J = 12.3$ Hz, 1H), 3.38–3.31 (m, 2H), 2.48 (s, 3H), 2.26 (s, 3H), 1.67–1.56 (m, 2H), 1.41–1.19 (m, 18H), 0.88 ppm (t, $J = 6.4$ Hz, 3H); IR (neat): $\tilde{\nu} = 3202$, 2916, 2847, 1651, 1605, 1582 cm^{-1}; ESI-MS *m/z*: 296 $[M+H]^+$; Anal. calcd for $C_{18}H_{33}NO_2$: C 73.17, H 11.26, N 4.74, found: C 73.33, H 11.28, N 4.75.

3-((Tridecylamino)methylene)pentane-2,4-dione (8b, EML322): Low-melting-point pale-yellow solid (303 mg, 98%): ^1H NMR (300 MHz, $CDCl_3$): $\delta = 11.07$ (br s, 1H), 7.72 (d, $J = 13.7$ Hz, 1H), 3.41–3.29 (m, 2H), 2.48 (s, 3H), 2.24 (s, 3H), 1.68–1.58 (m, 2H), 1.34–1.19 (m, 20H), 0.88 ppm (t, $J = 6.5$ Hz, 3H); ^{13}C NMR (75 MHz, $CDCl_3$): $\delta = 200.4$, 194.4, 160.0, 111.5, 50.6, 32.0, 30.7, 29.8, 29.6, 29.5, 29.3, 27.5, 26.6, 22.8, 14.2 ppm; IR (neat): $\tilde{\nu} = 3202$, 2916, 2851, 1651, 1605, 1585 cm^{-1}; ESI-MS *m/z*: 310 $[M+H]^+$; Anal. calcd for $C_{19}H_{35}NO_2$: C 73.74, H 11.40, N 4.53, found: C 73.94, H 11.42, N 4.54.

3-((Dodecyl(ethyl)amino)methylene)pentane-2,4-dione (8c, EML323): Low-melting-point pale-yellow solid (301 mg, 93%): ^1H NMR (300 MHz, $CDCl_3$): $\delta = 7.36$ (s, 1H), 3.32–3.20 (m, 4H), 2.32 (s, 6H), 1.58–1.42 (m, 2H), 1.33–1.20 (m, 18H), 1.19–1.03 (m, 3H), 0.87 ppm (t, $J = 6.3$ Hz, 3H); IR (neat): $\tilde{\nu} = 2924$, 2855, 1655, 1620, 1578 cm^{-1}; ESI-MS *m/z*: 324 $[M+H]^+$; Anal. calcd for $C_{20}H_{37}NO_2$: C 74.25, H 11.53, N 4.33, found: C 74.47, H 11.55, N 4.34.

3-((Ethyl(tridecyl)amino)methylene)pentane-2,4-dione (8d, EML324): Low-melting-point pale-yellow solid (317 mg, 94%): ^1H NMR (300 MHz, $CDCl_3$): $\delta = 7.36$ (s, 1H), 3.39–3.18 (m, 4H), 2.32 (s, 6H), 1.62–1.37 (m, 2H), 1.35–1.19 (m, 20H), 1.18–1.05 (m, 3H), 0.87 ppm (t, $J = 6.4$ Hz, 3H); IR (neat): $\tilde{\nu} = 2920$, 2851, 1659, 1612, 1578 cm^{-1}; ESI-MS *m/z*: 338 $[M+H]^+$; Anal. calcd for $C_{21}H_{39}NO_2$: C 74.72, H 11.65, N 4.15, found: C 74.94, H 11.68, N 4.16.

3-((Benzyl(dodecyl)amino)methylene)pentane-2,4-dione (8e, EML325): Pale-yellow solid (370 mg, 96%): mp: 53–56 °C; ^1H NMR (300 MHz, $CDCl_3$): $\delta = 7.49$ (s, 1H), 7.38–7.27 (m, 3H), 7.18–7.10 (m, 2H), 4.44 (s, 2H), 3.37–3.20 (m, 2H), 2.15 (s, 6H), 1.62–1.46 (m, 2H), 1.32–1.19 (m, 18H), 0.88 ppm (t, $J = 6.5$ Hz, 3H); IR (neat): $\tilde{\nu} = 2916$, 2851, 1670, 1574 cm^{-1}; ESI-MS *m/z*: 386 $[M+H]^+$; Anal. calcd for $C_{25}H_{39}NO_2$: C 77.87, H 10.20, N 3.63, found: C 78.10, H 10.22, N 3.64.

3-((Benzyl(tridecyl)amino)methylene)pentane-2,4-dione (8f, EML326): Pale-yellow solid (388 mg, 97%): mp: 61–64 °C; ^1H NMR (300 MHz, $CDCl_3$): $\delta = 7.49$ (s, 1H), 7.39–7.28 (m, 3H), 7.20–7.11 (m, 2H), 4.43 (s, 2H), 3.34–3.17 (m, 2H), 2.15 (s, 6H), 1.66–1.48 (m, 2H), 1.31–1.20 (m, 20H), 0.88 ppm (t, $J = 6.4$ Hz, 3H); IR (neat): $\tilde{\nu} = 2916$, 2851, 1674, 1574 cm^{-1}; ESI-MS *m/z*: 400 $[M+H]^+$; Anal. calcd for $C_{26}H_{41}NO_2$: C 78.15, H 10.34, N 3.51, found: C 78.38, H 10.36, N 3.52.

Surface plasmon resonance

SPR analyses were performed with a Biacore 3000 optical biosensor equipped with research-grade CM5 sensor chips (Biacore AB). Recombinant p300/KAT3B (Enzo Life Sciences, cat.# BML-SE451; GenBank accession no. NM001429) and PCAF/KAT2B (Biovision, cat.# 1137–100; GenBank accession n. NM003884) HAT domains were used in this analysis. Proteins (10 $\mu g\,mL^{-1}$ in 100 mM sodium acetate, pH 4.5) were immobilized on individual flow cells of the

sensor chip at a flow rate of 10 μL min^{-1} using standard amine coupling protocols to obtain densities of 8–9 kRU. Myoglobin was used as a negative control, and one flow cell was left empty for background subtraction. Compounds **2**–**8** were dissolved in DMSO (100%) to obtain 50 mM solutions, and they were diluted in HBS-P (10 mM HEPES pH 7.4, 0.15 M NaCl, 0.005% surfactant P20) while maintaining a final 0.2% DMSO concentration. Binding experiments were performed at 25 °C using a flow rate of 30 μL min^{-1} with 120 s association monitoring and 200 s dissociation monitoring. Surface regeneration was performed when necessary by a 10 s injection of 5 mM NaOH. The simple 1:1 Langmuir binding fit model of BIAevaluation software (version 4.1) was used for determining equilibrium dissociation constants (K_D) and kinetic dissociation (k_d) and association (k_a) constants using Equations (1) and (2), where R represents the response unit, and C is the concentration of the analyte.

$$\frac{dR}{dt} = k_a C(R_{max} - R) - k_d R \quad (1)$$

$$K_D = k_d / k_a \quad (2)$$

Biological methods

Histone acetyl transferase IC_{50} profiling: The effect of the test derivatives on the catalytic activity of PCAF and p300 was determined with a HotSpot HAT activity assay by Reaction Biology Corporation (Malvern, PA, USA) according to the company's standard operating procedure. Briefly, the recombinant catalytic domains of PCAF (aa 492–658) or p300 (aa 1284–1673) were incubated with histone H3 as a substrate (5 μM) and [acetyl-^{3}H]-acetyl coenzyme A (3.08 μM) as an acetyl donor in reaction buffer (50 mM Tris-HCl (pH 8.0), 50 mM NaCl, 0.1 mM EDTA, 1 mM DTT, 1 mM PMSF, 1% DMSO) for 1 h at 30 °C in the presence or absence of a dose titration of the compounds. Histone H3 acetylation was assessed by liquid scintillation. Anacardic acid or curcumin served as controls that inhibit PCAF or p300 activity, respectively. Data were analyzed using Excel and GraphPad Prism software (version 6.0, GraphPad Software Inc., San Diego, CA, USA) for IC_{50} curve fits using sigmoidal dose–response (variable slope) equations.

Cell viability assay: The U937 cell line (derived from a human histocytic lymphoma) was cultured in RPMI-1640 medium (Sigma) supplemented with 10% (*v*/*v*) fetal bovine serum (Sigma), 100 U mL^{-1} penicillin, and 100 μg mL^{-1} streptomycin (Sigma) at 37 °C in a 5% CO_2 atmosphere. U937 cell viability was measured via a 3-(4,5-dimethylthiazol-2-yl)-2,5-diphenyltetrazolium bromide (MTT) assay. A total of 100 μL of cells seeded in 96-well microtiter plates (2.5×10^5 cells mL^{-1}) were exposed for 24 h to different concentrations of selected compounds, ranging from 1 to 200 μM, in media containing 0.4% DMSO. The mitochondrial-dependent reduction of MTT to formazan was used to assess cell viability. Experiments were performed in quadruplicate, and all values are expressed as the percentage of the control containing 0.4% DMSO.

Cell-cycle analysis: For cell-cycle analysis, 250 μL of U937 cells (2.5×10^5 cells mL^{-1}) were seeded in 48-well plates and incubated with selected compounds at different concentrations. After 24 h of treatment, 250 μL of hypotonic buffer (33 mM sodium citrate, 0.1% Triton X-100, 50 μg mL^{-1} propidium iodide) was added to cell suspensions. Cells were analyzed with a FACScan flow cytometer (Becton Dickinson, CA), using Mod FitLT (version 3.2, Verity Software House, Inc., ME, USA) for quantitative analysis of cell-cycle distribution. All experiments were performed at least in triplicate.

Western blot analysis of acetyl-lysines: U937 (10 mL, 2.5×10^5 cells mL^{-1}), HeLa and C33A (sub-confluent) cells were seeded and incubated with compounds **2d**, **4b**, and **5b** at different concentrations, and after 24 h, the cells were harvested and washed three times with 1×PBS (Sigma) and then resuspended in lysis buffer (10 mM Tris pH 8, 1 mM KCl, 1.5 mM $MgCl_2$, and 1 mM DTT) supplemented with a protease inhibitor cocktail (Sigma). All subsequent manipulations were performed at 4 °C. After incubation for 1 h on a rotator, nuclei were collected by centrifugation for 10 min at 10000 *g*. The nuclear pellets were suspended in 0.4 N H_2SO_4, and after incubation for 2 h, were centrifuged for 15 min at 12000 *g*. Histones contained in the supernatant were precipitated by adding TCA to a final concentration of 33% and incubating overnight at 4 °C. After centrifugation at 10000 *g* for 30 min, the histone pellets were washed twice with acetone, air-dried, and finally redissolved in 50 μL of water. Protein concentrations were determined using the Bradford assay, and 1 μg of histones from each sample was loaded onto a 15% SDS-PAGE gel and transferred to a nitrocellulose membrane. The following primary antibodies were used: anti-Ac-histone H4 (Ser1/Lys5/Lys8/Lys12) (Santa Cruz cat.# sc-34263); anti-histone H4 (acetyl K5) (Abcam cat.# ab61236); anti-histone H3 (acetyl K9) (Abcam cat.# ab10812); anti-histone H3 (Abcam cat.# ab1791).

Acknowledgements

This study was supported by grants from the Italian Ministero dell'Istruzione, dell'Università e della Ricerca (MIUR)–Progetti di Ricerca di Interesse Nazionale (PRIN 2009PX2T2E, PRIN 20103W4779, and PRIN 2012ZHN9YH), the Italian Ministero dell'Istruzione, dell'Università e della Ricerca (MIUR)–Futuro in Ricerca (RBFR10ZJQT), the European Union's Seventh Framework Programme (FP7 BLUEPRINT/282510 and FP7 COST/TD0905), the Università di Salerno (Italy), and the Sapienza–Istituto Italiano di Tecnologia (ITT) Project. C.M. and M.V. were supported by the Università di Salerno with postdoctoral research fellowships, and A.F. by a predoctoral fellowship. The authors thank Dr. Kurumi Horiuchi (Reaction Biology Corporation) for helpful discussions.

Keywords: epigenetics · lysine acetyltransferases · PCAF activators · structure–activity relationships · surface plasmon resonance

[1] V. G. Allfrey, R. Faulkner, A. E. Mirsky, *Proc. Natl. Acad. Sci. USA* **1964**, *51*, 786–794.
[2] a) T. Kouzarides, *Cell* **2007**, *128*, 693–705; b) S. L. Berger, *Nature* **2007**, *447*, 407–412.
[3] a) A. J. Ruthenburg, H. Li, D. J. Patel, C. D. Allis, *Nat. Rev. Mol. Cell Biol.* **2007**, *8*, 983–994; b) B. D. Strahl, C. D. Allis, *Nature* **2000**, *403*, 41–45.
[4] T. Jenuwein, C. D. Allis, *Science* **2001**, *293*, 1074–1080.
[5] X.-J. Yang, E. Seto, *Mol. Cell* **2008**, *31*, 449–461.
[6] C. Choudhary, C. Kumar, F. Gnad, M. L. Nielsen, M. Rehman, T. C. Walther, J. V. Olsen, M. Mann, *Science* **2009**, *325*, 834–840.
[7] Y. Liu, A. L. Colosimo, X.-J. Yang, D. Liao, *Mol. Cell. Biol.* **2000**, *20*, 5540–5553.
[8] a) C. Hubbert, A. Guardiola, R. Shao, Y. Kawaguchi, A. Ito, A. Nixon, M. Yoshida, X.-F. Wang, T.-P. Yao, *Nature* **2002**, *417*, 455–458; b) J. S. Akella, D. Wloga, J. Kim, N. G. Starostina, S. Lyons-Abbott, N. S. Morrissette, S. T. Dougan, E. T. Kipreos, J. Gaertig, *Nature* **2010**, *467*, 218–222.
[9] M. A. Glozak, N. Sengupta, X. Zhang, E. Seto, *Gene* **2005**, *363*, 15–23.

[10] a) P. Matthias, M. Yoshida, S. Khochbin, *Cell Cycle* **2008**, *7*, 7 – 10; b) X.-J. Yang, E. Seto, *Nat. Rev. Mol. Cell Biol.* **2008**, *9*, 206 – 218; c) M. Arif, B. R. Selvi, T. K. Kundu, *ChemBioChem* **2010**, *11*, 1501 – 1504.

[11] a) M. von Wantoch Rekowski, A. Giannis, *Biochim. Biophys. Acta Gene Regul. Mech.* **2010**, *1799*, 760 – 767; b) S. Zhao, W. Xu, W. Jiang, W. Yu, Y. Lin, T. Zhang, J. Yao, L. Zhou, Y. Zeng, H. Li, Y. Li, J. Shi, W. An, S. M. Hancock, F. He, L. Qin, J. Chin, P. Yang, X. Chen, Q. Lei, Y. Xiong, K.-L. Guan, *Science* **2010**, *327*, 1000 – 1004; c) Q. Wang, Y. Zhang, C. Yang, H. Xiong, Y. Lin, J. Yao, H. Li, L. Xie, W. Zhao, Y. Yao, Z.-B. Ning, R. Zeng, Y. Xiong, K.-L. Guan, S. Zhao, G.-P. Zhao, *Science* **2010**, *327*, 1004 – 1007.

[12] C. D. Allis, S. L. Berger, J. Cote, S. Dent, T. Jenuwien, T. Kouzarides, L. Pillus, D. Reinberg, Y. Shi, R. Shiekhattar, A. Shilatifard, J. Workman, Y. Zhang, *Cell* **2007**, *131*, 633 – 636.

[13] Lysine acetylation was initially identified in histones, so many KATs and KDACs are often referred to as histone acetyltransferases (HATs) and deacetylases (HDACs), respectively.

[14] a) F. J. Dekker, H. J. Haisma, *Drug Discov. Today* **2009**, *14*, 942 – 948; b) F. Manzo, F. P. Tambaro, A. Mai, L. Altucci, *Expert Opin. Ther. Pat.* **2009**, *19*, 761 – 774; c) S. D. Furdas, S. Kannan, W. Sippl, M. Jung, *Arch. Pharm.* **2012**, *345*, 7 – 21.

[15] a) A. Mai, S. Massa, D. Rotili, I. Cerbara, S. Valente, R. Pezzi, S. Simeoni, R. Ragno, *Med. Res. Rev.* **2005**, *25*, 261 – 309; b) S. Minucci, P. G. Pelicci, *Nat. Rev. Cancer* **2006**, *6*, 38 – 51.

[16] V. M. Richon, S. Emiliani, E. Verdin, Y. Webb, R. Breslow, R. A. Rifkind, P. A. Marks, *Proc. Natl. Acad. Sci. USA* **1998**, *95*, 3003 – 3007.

[17] H. Nakajima, Y. B. Kim, H. Terano, M. Yoshida, S. Horinouchi, *Exp. Cell Res.* **1998**, *241*, 126 – 133.

[18] a) Z. Nagy, L. Tora, *Oncogene* **2007**, *26*, 5341 – 5357; b) R. Marmorstein, R. C. Trievel, *Biochim. Biophys. Acta Gene Regul. Mech.* **2009**, *1789*, 58 – 68; c) K. K. Lee, J. L. Workman, *Nat. Rev. Mol. Cell Biol.* **2007**, *8*, 284 – 295; d) S. C. Hodawadekar, R. Marmorstein, *Oncogene* **2007**, *26*, 5528 – 5540; e) K. Sadoul, J. Wang, B. Diagouraga, S. Khochbin, *J. Biomed. Biotechnol.* **2011**, *2011*, 970382.

[19] a) L. Howe, D. Auston, P. Grant, S. John, R. G. Cook, J. L. Workman, L. Pillus, *Genes Dev.* **2001**, *15*, 3144 – 3154; b) S. A. Gayther, S. J. Batley, L. Linger, A. Bannister, K. Thorpe, S.-F. Chin, Y. Daigo, P. Russell, A. Wilson, H. M. Sowter, J. D. A. Delhanty, B. A. J. Ponder, T. Kouzarides, C. Caldas, *Nat. Genet.* **2000**, *24*, 300 – 303; c) D. Bandyopadhyay, N. A. Okan, E. Bales, L. Nascimento, P. A. Cole, E. E. Medrano, *Cancer Res.* **2002**, *62*, 6231 – 6239; d) A. Giordano, M. L. Avantaggiati, *J. Cell. Physiol.* **1999**, *181*, 218 – 230; e) S. Pfister, S. Rea, M. Taipale, F. Mendrzyk, B. Straub, C. Ittrich, O. Thuerigen, H. P. Sinn, A. Akhtar, P. Lichter, *Int. J. Cancer* **2008**, *122*, 1207 – 1213; f) T. Katsumoto, N. Yoshida, I. Kitabayashi, *Cancer Sci.* **2008**, *99*, 1523 – 1527; g) N. G. Iyer, J. Xian, S. F. Chin, A. J. Bannister, Y. Daigo, S. Aparicio, T. Kouzarides, C. Caldas, *Oncogene* **2007**, *26*, 21 – 29; h) I. Kitabayashi, Y. Aikawa, A. Yokoyama, F. Hosoda, M. Nagai, N. Kakazu, T. Abe, M. Ohki, *Leukemia* **2001**, *15*, 89 – 94; i) S. Ait-Si-Ali, A. Polesskaya, S. Filleur, R. Ferreira, A. Duquet, P. Robin, A. Vervish, D. Trouche, F. Cabon, A. Harel-Bellan, *Oncogene* **2000**, *19*, 2430 – 2437; j) N. Reynoird, B. E. Schwartz, M. Delvecchio, K. Sadoul, D. Meyers, C. Mukherjee, C. Caron, H. Kimura, S. Rousseaux, P. A. Cole, D. Panne, C. A. French, S. Khochbin, *EMBO J.* **2010**, *29*, 2943 – 2952.

[20] a) I. M. Adcock, L. Tsaprouni, P. Bhavsar, K. Ito, *Curr. Opin. Immunol.* **2007**, *19*, 694 – 700; b) X. J. Yang, *Nucleic Acids Res.* **2004**, *32*, 959 – 976; c) K. Mantelingu, B. A. A. Reddy, V. Swaminathan, A. H. Kishore, N. B. Siddappa, G. V. P. Kumar, G. Nagashankar, N. Natesh, S. Roy, P. P. Sadhale, U. Ranga, C. Narayana, T. K. Kundu, *Chem. Biol.* **2007**, *14*, 645 – 657; d) P. J. Barnes, I. M. Adcock, K. Ito, *Eur. Respir. J.* **2005**, *25*, 552 – 563; e) P. J. Barnes, *Proc. Am. Thorac. Soc.* **2009**, *6*, 693 – 696; f) H.-H. Cheng, K.-H. Wang, L.-y. Chu, T.-C. Chang, C.-C. Kuo, K. K. Wu, *PLoS ONE* **2014**, *9*, e88507.

[21] L. Liu, X. T. Zhen, E. Denton, B. D. Marsden, M. Schapira, *Bioinformatics* **2012**, *28*, 2205 – 2206.

[22] a) C. Colussi, A. Scopece, S. Vitale, F. Spallotta, S. Mattiussi, J. Rosati, B. Illi, A. Mai, S. Castellano, G. Sbardella, A. Farsetti, M. C. Capogrossi, C. Gaetano, *Arterioscler. Thromb. Vasc. Biol.* **2012**, *32*, 2435 – 2443; b) C. Colussi, J. Rosati, S. Straino, F. Spallotta, R. Berni, D. Stilli, S. Rossi, E. Musso, E. Macchi, A. Mai, G. Sbardella, S. Castellano, C. Chimenti, A. Frustaci, A. Nebbioso, L. Altucci, M. C. Capogrossi, C. Gaetano, *Proc. Natl. Acad. Sci. USA* **2011**, *108*, 2795 – 2800; c) M. Vecellio, F. Spallotta, S. Nanni, C. Colussi, C. Cencioni, A. Derlet, B. Bassetti, M. Tilenni, M. C. Carena, A. Farsetti, G. Sbardella, S. Castellano, A. Mai, F. Martelli, G. Pompilio, M. C. Capogrossi, A. Rossini, S. Dimmeler, A. M. Zeiher, C. Gaetano, *Diabetes* **2014**, *63*, 2132 – 2147.

[23] a) O. D. Lau, T. K. Kundu, R. E. Soccio, S. Ait-Si-Ali, E. M. Khalil, A. Vassilev, A. P. Wolffe, Y. Nakatani, R. G. Roeder, P. A. Cole, *Mol. Cell* **2000**, *5*, 589 – 595; b) R. N. Saha, K. Pahan, *Cell Death Differ.* **2006**, *13*, 539 – 550; c) C. Rouaux, N. Jokic, C. Mbebi, S. Boutillier, J.-P. Loeffler, A.-L. Boutillier, *EMBO J.* **2003**, *22*, 6537 – 6549; d) R. M. Barrett, M. A. Wood, *Learn. Mem.* **2008**, *15*, 460 – 467; e) T. Maurice, F. Duclot, J. Meunier, G. Naert, L. Givalois, J. Meffre, A. Celerier, C. Jacquet, V. Copois, N. Mechti, K. Ozato, C. Gongora, *Neuropsychopharmacology* **2008**, *33*, 1584 – 1602; f) W. Wei, C. M. Coelho, X. Li, R. Marek, S. Yan, S. Anderson, D. Meyers, C. Mukherjee, G. Sbardella, S. Castellano, C. Milite, D. Rotili, A. Mai, P. A. Cole, P. Sah, M. S. Kobor, T. W. Bredy, *J. Neurosci.* **2012**, *32*, 11930 – 11941; g) F. Duclot, J. Meffre, C. Jacquet, C. Gongora, T. Maurice, *Neuroscience* **2010**, *167*, 850 – 863.

[24] a) B. R. Stockwell, *Nat. Rev. Genet.* **2000**, *1*, 116 – 125; b) E. M. Bowers, G. Yan, C. Mukherjee, A. Orry, L. Wang, M. A. Holbert, N. T. Crump, C. A. Hazzalin, G. Liszczak, H. Yuan, C. Larocca, S. A. Saldanha, R. Abagyan, Y. Sun, D. J. Meyers, R. Marmorstein, L. C. Mahadevan, R. M. Alani, P. A. Cole, *Chem. Biol.* **2010**, *17*, 471 – 482.

[25] M. Cebrat, C. M. Kim, P. R. Thompson, M. Daugherty, P. A. Cole, *Bioorg. Med. Chem.* **2003**, *11*, 3307 – 3313.

[26] K. Balasubramanyam, V. Swaminathan, A. Ranganathan, T. K. Kundu, *J. Biol. Chem.* **2003**, *278*, 19134 – 19140.

[27] K. Balasubramanyam, M. Altaf, R. A. Varier, V. Swaminathan, A. Ravindran, P. P. Sadhale, T. K. Kundu, *J. Biol. Chem.* **2004**, *279*, 33716 – 33726.

[28] K. Balasubramanyam, R. A. Varier, M. Altaf, V. Swaminathan, N. B. Siddappa, U. Ranga, T. K. Kundu, *J. Biol. Chem.* **2004**, *279*, 51163 – 51171.

[29] K. C. Ravindra, B. R. Selvi, M. Arif, B. A. A. Reddy, G. R. Thanuja, S. Agrawal, S. K. Pradhan, N. Nagashayana, D. Dasgupta, T. K. Kundu, *J. Biol. Chem.* **2009**, *284*, 24453 – 24464.

[30] F. Dal Piaz, A. Tosco, D. Eletto, A. L. Piccinelli, O. Moltedo, S. Franceschelli, G. Sbardella, P. Remondelli, L. Rastrelli, L. Vesci, C. Pisano, N. De Tommasi, *ChemBioChem* **2010**, *11*, 818 – 827.

[31] a) E. D. Eliseeva, V. Valkov, M. Jung, M. O. Jung, *Mol. Cancer Ther.* **2007**, *6*, 2391 – 2398; b) M. Ghizzoni, A. Boltjes, C. de Graaf, H. J. Haisma, F. J. Dekker, *Bioorg. Med. Chem.* **2010**, *18*, 5826 – 5834; c) J. A. Souto, M. Conte, R. Álvarez, A. Nebbioso, V. Carafa, L. Altucci, A. R. de Lera, *ChemMedChem* **2008**, *3*, 1435 – 1442; d) R. Costi, R. Di Santo, M. Artico, G. Miele, P. Valentini, E. Novellino, A. Cereseto, *J. Med. Chem.* **2007**, *50*, 1973 – 1977; e) A. Mai, D. Cheng, M. T. Bedford, S. Valente, A. Nebbioso, A. Perrone, G. Brosch, G. Sbardella, F. De Bellis, M. Miceli, L. Altucci, *J. Med. Chem.* **2008**, *51*, 2279 – 2290; f) M. Arif, B. M. Vedamurthy, R. Choudhari, Y. B. Ostwal, K. Mantelingu, G. S. Kodaganur, T. K. Kundu, *Chem. Biol.* **2010**, *17*, 903 – 913.

[32] M. D. Vasudevarao, P. Mizar, S. Kumari, S. Mandal, S. Siddhanta, M. M. M. Swamy, S. Kaypee, R. C. Kodihalli, A. Banerjee, C. Narayana, D. Dasgupta, T. K. Kundu, *J. Biol. Chem.* **2014**, *289*, 7702 – 7717.

[33] a) L. Stimson, M. G. Rowlands, Y. M. Newbatt, N. F. Smith, F. I. Raynaud, P. Rogers, V. Bavetsias, S. Gorsuch, M. Jarman, A. Bannister, T. Kouzarides, E. McDonald, P. Workman, G. W. Aherne, *Mol. Cancer Ther.* **2005**, *4*, 1521 – 1532; b) S. Gorsuch, V. Bavetsias, M. G. Rowlands, G. W. Aherne, P. Workman, M. Jarman, E. McDonald, *Bioorg. Med. Chem.* **2009**, *17*, 467 – 474; c) M. Ghizzoni, H. J. Haisma, F. J. Dekker, *Eur. J. Med. Chem.* **2009**, *44*, 4855 – 4861; d) F. J. Dekker, M. Ghizzoni, N. van der Meer, R. Wisastra, H. J. Haisma, *Bioorg. Med. Chem.* **2009**, *17*, 460 – 466.

[34] S. D. Furdas, S. Shekfeh, E.-M. Bissinger, J. M. Wagner, S. Schlimme, V. Valkov, M. Hendzel, M. Jung, W. Sippl, *Bioorg. Med. Chem.* **2011**, *19*, 3678 – 3689.

[35] B. M. Dancy, N. T. Crump, D. J. Peterson, C. Mukherjee, E. M. Bowers, Y.-H. Ahn, M. Yoshida, J. Zhang, L. C. Mahadevan, D. J. Meyers, J. D. Boeke, P. A. Cole, *ChemBioChem* **2012**, *13*, 2113 – 2121.

[36] M. Biel, A. Kretsovali, E. Karatzali, J. Papamatheakis, A. Giannis, *Angew. Chem. Int. Ed.* **2004**, *43*, 3974 – 3976; *Angew. Chem.* **2004**, *116*, 4065 – 4067.

[37] a) A. Mai, D. Rotili, D. Tarantino, P. Ornaghi, F. Tosi, C. Vicidomini, G. Sbardella, A. Nebbioso, M. Miceli, L. Altucci, P. Filetici, *J. Med. Chem.* **2006**, *49*, 6897 – 6907; b) A. Lenoci, S. Tomassi, M. Conte, R. Benedetti, V. Rodriguez, S. Carradori, D. Secci, S. Castellano, G. Sbardella, P. Filetici, E. Novellino, L. Altucci, D. Rotili, A. Mai, *ChemMedChem* **2014**, *9*, 542 – 548.

[38] J. A. Souto, R. Benedetti, K. Otto, M. Miceli, R. Álvarez, L. Altucci, A. R. de Lera, *ChemMedChem* **2010**, *5*, 1530 – 1540.
[39] a) C. Milite, S. Castellano, R. Benedetti, A. Tosco, C. Ciliberti, C. Vicidomini, L. Boully, G. Franci, L. Altucci, A. Mai, G. Sbardella, *Bioorg. Med. Chem.* **2011**, *19*, 3690 – 3701; b) G. Sbardella, S. Castellano, C. Vicidomini, D. Rotili, A. Nebbioso, M. Miceli, L. Altucci, A. Mai, *Bioorg. Med. Chem. Lett.* **2008**, *18*, 2788 – 2792.
[40] Samples of compound SPV106 and any other chemical probe described herein can be provided for scientific collaboration. The authors are committed to making them freely available without restriction for any research purpose.
[41] F. Spallotta, C. Cencioni, S. Straino, G. Sbardella, S. Castellano, M. C. Capogrossi, F. Martelli, C. Gaetano, *Commun. Integr. Biol.* **2013**, *6*, e25466.
[42] S. Castellano, A. Spannhoff, C. Milite, F. Dal Piaz, D. Cheng, A. Tosco, M. Viviano, A. Yamani, A. Cianciulli, M. Sala, V. Cura, J. Cavarelli, E. Novellino, A. Mai, M. T. Bedford, G. Sbardella, *J. Med. Chem.* **2012**, *55*, 9875 – 9890.
[43] C. Milite, M. Viviano, M. Santoriello, F. Arico, G. Sbardella, S. Castellano, *RSC Adv.* **2012**, *2*, 5229 – 5233.
[44] Derivative **2 d** was previously reported by us; see Ref. [lit39 > a].
[45] Derivative **3 a** was previously reported; see: "Preparation of 3-Carboalkoxy or 3-Alkanoyl Furans", R. A. Kretchmer, R. A. Laitar, US Patent No. US 4025537 A, **1977**; R. A. Kretchmer, R. A. Laitar, *J. Org. Chem.* **1978**, *43*, 4596 – 4598.
[46] Derivative **8 a** was previously reported; see: "N-Substituted 2-Aminovinyl Compounds, their Preparation and their Use as Lightscreens", M. Kuhn, P. Ouziel, (Ciba-Geigy AG, Basel, Switzerland), German Patent No. DE3825382 A1, **1989**.
[47] P. Černuchová, G. Vo-Thanh, V. Milata, A. Loupy, *Heterocycles* **2004**, *64*, 177 – 191.
[48] C. E. Berndsen, J. M. Denu, *Methods* **2005**, *36*, 321 – 331.
[49] I. Navratilova, A. L. Hopkins, *ACS Med. Chem. Lett.* **2010**, *1*, 44 – 48.
[50] G. LeRoy, P. DiMaggio, E. Chan, B. Zee, M. Blanco, B. Bryant, I. Flaniken, S. Liu, Y. Kang, P. Trojer, B. Garcia, *Epigenet. Chromatin* **2013**, *6*, 20.
[51] I. Nicoletti, G. Migliorati, M. C. Pagliacci, F. Grignani, C. Riccardi, *J. Immunol. Methods* **1991**, *139*, 271 – 279.
[52] a) X.-n. Gao, J. Lin, Q.-y. Ning, L. Gao, Y.-s. Yao, J.-h. Zhou, Y.-h. Li, L.-l. Wang, L. Yu, *PLoS ONE* **2013**, *8*, e55481; b) F. Mateo, M. Vidal-Laliena, N. Canela, A. Zecchin, M. Martínez-Balbás, N. Agell, M. Giacca, M. J. Pujol, O. Bachs, *Nucleic Acids Res.* **2009**, *37*, 7072 – 7084; c) P.-C. Sun, C. Tzao, B.-H. Chen, C.-W. Liu, C.-P. Yu, J.-S. Jin, *J. Biomed. Sci.* **2010**, *17*, 76; d) M.-Z. Ying, J.-J. Wang, D.-W. Li, G.-Z. Yu, X. Wang, J. Pan, Y. Chen, M.-X. He, *Cancer Biol. Ther.* **2010**, *9*, 312 – 320; e) X. Zhao, W. Yang, C. Shi, W. Ma, J. Liu, Y. Wang, G. Jiang, *Tumor Biol.* **2011**, *32*, 335 – 346.
[53] In Figure 8 and in the text we used "Brno nomenclature" to indicate specific acetylation sites; see also: B. M. Turner, *Nat. Struct. Mol. Biol.* **2005**, *12*, 110 – 112.
[54] A. N. Poux, M. Cebrat, C. M. Kim, P. A. Cole, R. Marmorstein, *Proc. Natl. Acad. Sci. USA* **2002**, *99*, 14065 – 14070.
[55] X. Liu, L. Wang, K. Zhao, P. R. Thompson, Y. Hwang, R. Marmorstein, P. A. Cole, *Nature* **2008**, *451*, 846 – 850.
[56] P. A. Cole, *Nat. Chem. Biol.* **2008**, *4*, 590 – 597.
[57] M. Delvecchio, J. Gaucher, C. Aguilar-Gurrieri, E. Ortega, D. Panne, *Nat. Struct. Mol. Biol.* **2013**, *20*, 1040 – 1046.
[58] S. Shi, J. Lin, Y. Cai, J. Yu, H. Hong, K. Ji, J. Downey, X. Lu, R. Chen, J. Han, A. Han, *BMC Struct. Biol.* **2014**, *14*, 2.

Received: September 1, 2014
Published online on ■■ ■■, 0000

Ups and downs: Chemical manipulation of the carbonyl functional groups of a series of analogues of diethyl pentadecylidenemalonate **1** (SPV106), a mixed inhibitor/activator of lysine acetyltransferases that we recently identified, yielded different activity profiles against KAT2B and KAT3B (pure KAT2B activator, pan-inhibitor, or mixed KAT2B activator/KAT3B inhibitor).

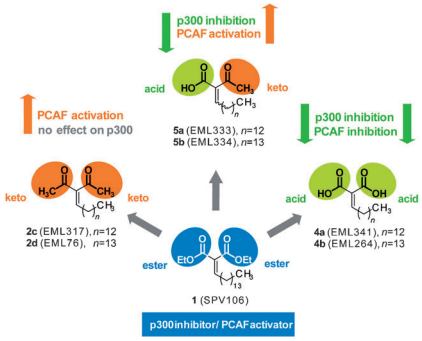

S. Castellano, C. Milite, A. Feoli, M. Viviano, A. Mai, E. Novellino, A. Tosco, G. Sbardella**

■■ – ■■

Identification of Structural Features of 2-Alkylidene-1,3-Dicarbonyl Derivatives that Induce Inhibition and/or Activation of Histone Acetyltransferases KAT3B/p300 and KAT2B/PCAF